

AD-A114 384

SYSTEMS RESEARCH LABS INC DAYTON OH
WIND-TUNNEL EVALUATION OF AN AEROELASTICALLY CONFORMABLE ROTOR. (1)

F/G 1/3

MAR 82 L R SUTTON, R P WHITE, R L MARKER

UNCLASSIFIED

USAAVRADCOM-TR-81-D-43

NL

1-1
A
20-1-82



END
DATE
FILMED
6 82
DTIC

USAAVRADCOM-TR-81-D-43



12

**WIND-TUNNEL EVALUATION OF AN AEROELASTICALLY
CONFORMABLE ROTOR**

Lawrence R. Sutton, Richard P. White, Jr., Robert L. Marker
SYSTEMS RESEARCH LABORATORIES, Inc.
2800 Indian Ripple Road
Dayton, Ohio 45440

March 1982

Final Report

Approved for public release;
distribution unlimited.

DTIC
SELECTED
MAY 11 1982
H

Prepared for
APPLIED TECHNOLOGY LABORATORY
U. S. ARMY RESEARCH AND TECHNOLOGY LABORATORIES (AVRADCOM)
Fort Eustis, Va. 23604

DTIC FILE COPY

82 05-10 108

APPLIED TECHNOLOGY LABORATORY POSITION STATEMENT

This report presents the results of a wind-tunnel evaluation of an Aeroelastically Conformable Rotor (ACR). The ACR is a rotor system for which the rotor blade mass and stiffness properties have been selected to encourage aeroelastic response which has a favorable effect on one or more rotor system characteristics such as power required or amplitude of vibratory forces transmitted to the fuselage. Sophisticated mathematical models were used to evaluate the effects of variations of rotor blade aeroelastic design properties compared to a relatively stiff baseline design. Model rotor blades for the baseline and ACR rotors were built and tested on a four-bladed articulated rotor model in two- and four-bladed configurations in the NASA/Langley Transonic Dynamic Tunnel.

This report concludes that the ACR concept can result in significant performance improvements at high values of thrust/solidity coefficient. Greater benefits would probably have been achieved if the desired torsional stiffness reduction had been obtained for the ACR model blades. Data presented regarding the effect of number of blades are not comprehensive enough for firm conclusions regarding the optimum number of blades for an ACR rotor.

Messrs. William E. Nettles and Edward E. Austin of the Aeronautical Technology Division served consecutively as project engineer for this effort. Mr. John H. Cline of the Structures Laboratory served as test engineer for the wind tunnel program.

DISCLAIMERS

The findings in this report are not to be construed as an official Department of the Army position unless so designated by other authorized documents.

When Government drawings, specifications, or other data are used for any purpose other than in connection with a definitely related Government procurement operation, the United States Government thereby incurs no responsibility nor any obligation whatsoever; and the fact that the Government may have formulated, furnished, or in any way supplied the said drawings, specifications, or other data is not to be regarded by implication or otherwise as in any manner licensing the holder or any other person or corporation, or conveying any rights or permission, to manufacture, use, or sell any patented invention that may in any way be related thereto.

Trade names cited in this report do not constitute an official endorsement or approval of the use of such commercial hardware or software.

DISPOSITION INSTRUCTIONS

Destroy this report when no longer needed. Do not return it to the originator.

Unclassified

SECURITY CLASSIFICATION OF THIS PAGE (When Data Entered)

REPORT DOCUMENTATION PAGE		READ INSTRUCTIONS BEFORE COMPLETING FORM
1. REPORT NUMBER USAAVRADCOM-TR-81-D-43	2. GOVT ACCESSION NO. A114 384	3. RECIPIENT'S CATALOG NUMBER
4. TITLE (and Subtitle) WIND-TUNNEL EVALUATION OF AN AEROELASTICALLY CONFORMABLE ROTOR		5. TYPE OF REPORT & PERIOD COVERED Final Report
		6. PERFORMING ORG. REPORT NUMBER
7. AUTHOR(s) Lawrence R. Sutton Richard P. White, Jr. Robert L. Marker		8. CONTRACT OR GRANT NUMBER(s) DAAJ02-77-C-0046
9. PERFORMING ORGANIZATION NAME AND ADDRESS Systems Research Laboratories, Inc. 2800 Indian Ripple Road Dayton, Ohio 45440		10. PROGRAM ELEMENT, PROJECT, TASK AREA & WORK UNIT NUMBERS 62209A 1L262209AH76 00 207 EK
11. CONTROLLING OFFICE NAME AND ADDRESS Applied Technology Laboratory, U.S. Army Research and Technology Laboratories (AVRADCOM) Fort Eustis, Virginia 23604		12. REPORT DATE March 1982
		13. NUMBER OF PAGES 86
14. MONITORING AGENCY NAME & ADDRESS (if different from Controlling Office)		15. SECURITY CLASS. (of this report) Unclassified
		15a. DECLASSIFICATION/DOWNGRADING SCHEDULE
16. DISTRIBUTION STATEMENT (of this Report) Approved for public release; distribution unlimited.		
17. DISTRIBUTION STATEMENT (of the abstract entered in Block 20, if different from Report)		
18. SUPPLEMENTARY NOTES		
19. KEY WORDS (Continue on reverse side if necessary and identify by block number) Helicopter Rotor Rotor Performance Dynamic Twist		
20. ABSTRACT (Continue on reverse side if necessary and identify by block number) This report summarizes the theoretical and experimental investigations that were conducted to evaluate the potential of aeroelastic and mass-elastic couplings in an aeroelastic conformable rotor (ACR) that will improve the performance and vibratory characteristics of helicopter rotor systems without creating instabilities. ACR parameters were identified and a baseline rotor system was selected. An ACR blade concept was investigated by altering the characteristics of the baseline and using automated analysis techniques. Model baseline and ACR blades were fabricated and underwent acceptance tests.		

DTIC
COLLECTED
MAY 11 1982
D
H

DD FORM 1 JAN 73 1473 EDITION OF 1 NOV 65 IS OBSOLETE

Unclassified

SECURITY CLASSIFICATION OF THIS PAGE (When Data Entered)

Unclassified

SECURITY CLASSIFICATION OF THIS PAGE(When Data Entered)

20. Abstract (cont'd)

→ Wind-tunnel testing was conducted to evaluate the benefits of the ACR design concept. It was demonstrated that the use of the ACR concept can result in significant performance improvements. ←

Unclassified

SECURITY CLASSIFICATION OF THIS PAGE(When Data Entered)

PREFACE

The work reported herein was performed by Systems Research Laboratories, Inc. (SRL) under Contract DAAJ02-77-C-0046, for the Applied Technology Laboratory (ATL), U.S. Army Research and Technology Laboratories (AVRADCOM), Ft. Eustis, Virginia. The work was carried out by Mr. Lawrence R. Sutton, Project Manager, with the technical supervision of Mr. Richard P. White Jr. and Mr. Robert L. Marker of the RASA Division of Systems Research Laboratories, Inc. The ATL technical monitors were consecutively Mr. William E. Nettles and Mr. Edward E. Austin. The Transonic Dynamics Tunnel test engineer was Mr. John H. Cline of the Structures Laboratory, Research and Technology Laboratories (AVRADCOM), NASA/Langley Research Center, Hampton Virginia.



Accession For	
NTIS GRA&I	<input checked="" type="checkbox"/>
DTIC TAB	<input type="checkbox"/>
Unannounced	<input type="checkbox"/>
Justification	
By _____	
Distribution/	
Availability Codes	
Avail and/or	
Dist	Special
A	

TABLE OF CONTENTS

<u>Section</u>	<u>Page</u>
PREFACE	3
LIST OF ILLUSTRATIONS	6
LIST OF TABLES	8
INTRODUCTION	9
PRELIMINARY INVESTIGATIONS	14
Selection of Primary ACR Parameters	14
Selection and Description of Analysis Techniques	16
Selection of Operational Qualities to be Improved	20
Selection of Basic Rotor Configuration	20
THEORETICAL INVESTIGATION OF ACR CONCEPT	22
Description of Computational Procedure	22
Results of the ACR Concept Studies	24
BLADE CONSTRUCTION	29
General Design Factors	29
Baseline Blade Design	42
ACR Blade Design	43
Stress Analysis	43
BLADE FABRICATION	46
Fabrication Process	46
Model Blade Characteristics	48
WIND-TUNNEL TESTS	55
Test Purposes and Procedures	55
Discussion of Experimental Results	57
THEORETICAL/EXPERIMENTAL CORRELATION	73
CONCLUSIONS AND RECOMMENDATIONS	76
REFERENCES	78
BIBLIOGRAPHY	80
LIST OF SYMBOLS	86

PRECEDING PAGE BLANK-NOT FILLED

LIST OF ILLUSTRATIONS

<u>Figure</u>	<u>Page</u>
1. Modal Frequency vs. Rotor RPM for Baseline Blade	26
2. Modal Frequency vs. Rotor RPM for ACR Swept-Tip Blade	27
3. Baseline Blade Analytical Model Flapwise Stiffness Distribution.	33
4. Baseline Blade Analytical Model Edgewise Stiffness Distribution.	34
5. Baseline Blade Analytical Model Torsional Stiffness Distribution.	35
6. Baseline Blade Analytical Model Mass and Weight per Inch Distribution	36
7. Distributions of Baseline Blade Analytical Model Center of Gravity and Shear Center Axis Offsets Relative to Blade Pitch Axis (at 25% Chord)	37
8. Baseline Blade Analytical Model Torsional Inertia Distribution.	38
9. Design Features of Baseline Blade	44
10. Design Features of ACR Blade.	45
11. Typical Balance Weight Installation	47
12. Balance Weight Attachment Test Setup.	47
13. Static Deflection (Spar) Test Setup	51
14. Vibration Test Setup.	52
15. ACR Swept-Tip Blades Mounted in the NASA Transonic Dynamics Tunnel	56
16. Coefficient of Thrust/Solidity Ratio vs. Coefficient of Power/Solidity Ratio - $\mu = 0.25$	58
17. Thrust Coefficient/Solidity Ratio vs. Power Coefficient Solidity Ratio - $\mu = 0.35$	59
18. C_T/C_Q vs. C_T/σ for Four-Bladed Rotors	62
19. Nondimensional Oscillatory Flapwise Bending Moment at 18% Radius vs. Thrust Coefficient/Solidity Ratio for $\mu = 0.25$	63
20. Nondimensional Oscillatory Flapwise Bending Moment at 18% Radius vs. Thrust Coefficient/Solidity Ratio for $\mu = 0.35$	64
21. Nondimensional Oscillatory Edgewise Bending Moment at 18% Radius vs. Thrust Coefficient/Solidity Ratio for $\mu = 0.25$	66
22. Nondimensional Oscillatory Edgewise Bending Moment at 18% Radius vs. Thrust Coefficient/Solidity Ratio for $\mu = 0.35$	67
23. Nondimensional Oscillatory Torsional Moment at 18% Radius vs. Thrust Coefficient/Solidity Ratio for $\mu = 0.25$	68

LIST OF ILLUSTRATIONS (continued)

<u>Figure</u>		<u>Page</u>
24.	Nondimensional Oscillatory Torsional Moment at 18% Radius vs. Thrust Coefficient/Solidity Ratio for $\mu = 0.35$	69
25.	Oscillatory Flapwise Bending Moment vs. C_T/σ for Two-Bladed Rotors	70
26.	Oscillatory Edgewise Bending Moment vs. C_T/σ for Two-Bladed Rotors	71
27.	Oscillatory Torsional Moment vs. C_T/σ for Two-Bladed Rotors	72

LIST OF TABLES

<u>Table</u>	<u>Page</u>
1. Predictive Analyses Evaluated for Possible Use in Program	17
2. Relative Performance Benefits of ACR Parameters	25
3. Degree of Damping Predicted for Various Modes	28
4. Summary of Rotor System Characteristics for the Analytical Scale Model and Full-Scale Rotor System	30
5. System Parameter Scale Factors for the Baseline Model Designed for Testing in Freon 12	30
6. Mass Elastic Properties of Baseline and ACR Blades	31
7. 17-4 PH (H1150) Stainless Steel Mechanical Properties	41
8. Baseline Blade Nonrotating Frequencies, Hz	53
9. Test Configurations	55
10. Predicted Results Using Measured Blade Properties	74

1
F

INTRODUCTION

The approach of dynamically altering the characteristics of rotor systems to provide control and relief from rotor dynamic loadings has been used since the beginning of helicopter flight. Examples of this approach are the use of cyclic pitch for control and relief of bending loads, flap hinges to relieve root bending moments and stresses, and lead-lag hinges to relieve blade inplane stresses. For two-bladed rotors, a teetering hinge has been generally used to relieve the blade root flapwise bending moments and to relieve rotor stability problems.

In an attempt to relieve the compressibility and stall problems simultaneously, a German company (Boelkow) used crossover beams between opposite blades, pinned in the lead-lag direction. When the increased drag torque produced on the advancing side rotated the advancing blade aft, this motion was transferred to the opposite blade through the crossover beams to increase its velocity in the third and fourth rotor quadrants. The increased velocity of the retreating blade decreased the angle-of-attack requirements and thus, the stall problems in these quadrants. While this approach was attractive on a performance basis, stability problems eliminated it from further serious consideration.

Other types of "mechanical" approaches have also been used to affect blade motions by reducing loadings and to provide beneficial couplings both for performance and stability considerations. Blade sweep, pitch-flap and flap-lag couplings are examples of types of mechanical couplings. While each of these mechanical couplings could be beneficial by itself, improper couplings of the independent parameters could also degrade performance, increase dynamic loadings and blade stresses, and in some cases, create stability problems. These passive mechanical approaches to develop a rotor system that would be adaptive to its operational environment, while providing significant benefits, were constrained to basically a modification of 1/rev effects.

In order to obtain possible performance and vibration reduction benefits associated with 2/rev and 4 rev tailoring of the blade angle-of-attack, a number of investigations have been conducted in the past regarding the use of higher harmonic mechanical pitch control (References 1 through 5).

1. Stewart, W., SECOND HARMONIC CONTROL OF THE HELICOPTER ROTOR, Aeronautical Research Council, R&M 2997, London, England, August 1952.
2. Arcidiacono, P. J., THEORETICAL PERFORMANCE OF HELICOPTERS HAVING SECOND AND HIGHER HARMONIC FEATHERING CONTROL, Journal of the American Helicopter Society, April 1961.
3. AN EXPERIMENTAL INVESTIGATION OF A SECOND HARMONIC FEATHERING DEVICE ON THE UH-1A HELICOPTER, Bell Helicopter Company; USATRECOM Technical Report 62-109, U.S. Army Transportation and Engineering Command, Ft. Eustis, Virginia, June 1963.

These studies indicated that benefits could be obtained, particularly in the reduction of rotor vibratory forces transmitted to the fuselage, but stability and mechanical problems reduced the desirability of these approaches at the time.

With the advent of rigid or hingeless types of rotor systems, other types of system dynamic couplings also became available due to the elasticity of the blades. For example, frequency tuning of the flap and lag stiffness of the blades was used to reduce blade oscillatory stresses as well as for the solution of stability problems associated with these types of rotor systems. Since pitch-flap, pitch-lag, and flap-lag couplings are obtained in these blades through elastic deformations instead of through the angular relationships of mechanical hinges, it might be said that these types of rotor systems in their rudimentary form are aeroelastically conformable rotors. These rotor systems, although having aeroplastic couplings, are constructed such that they basically use only the 1/rev or odd-order torque functions to provide passive control of the rotor blades. The effects of higher harmonic root pitch control on the performance, vibration, and stability characteristics of a hingeless rotor have also been studied (References 6 and 7). The results of these studies indicate that higher harmonic mechanical root pitch control can be beneficial as regards the performance and the transmitted vibratory characteristics of hingeless rotors.

4. Daughaday, H., SUPPRESSION OF TRANSMITTED HARMONIC ROTOR LOADS BY BLADE PITCH CONTROL, Cornell Aeronautical Laboratory, Inc. USAAVLABS Technical Report 67-14, U.S. Army Aviation Materiel Laboratories, Ft. Eustis, Virginia, November 1967, AD 665430.
5. Balcerak, J. C., and Erickson, J. C., SUPPRESSION OF TRANSMITTED HARMONIC VERTICAL AND INPLANE ROTOR LOADS BY BLADE PITCH CONTROL, Cornell Aeronautical Laboratory, Inc., USAAVLABS Technical Report 69-39, U.S. Army Aviation Material Laboratories, Ft. Eustis, Virginia, July 1969, AD 860352.
6. Sissingh, G. J., and Donham, R. E., HINGELESS ROTOR THEORY AND EXPERIMENT ON VIBRATION REDUCTION BY PERIODIC VARIATION OF CONVENTIONAL CONTROLS, Proceedings of the AHS/NASA/Ames Specialists' Meeting on Rotorcraft Dynamics, February 1974 (NASA SP 352, February 1974).
7. McHugh, Frank J., and Shaw, John, Jr., BENEFITS OF HIGHER HARMONIC BLADE PITCH: VIBRATION REDUCTION, BLADE-LOAD REDUCTION, AND PERFORMANCE IMPROVEMENT, American Helicopter Society Mid-East Region Symposium on Rotor Technology, August 1976.

All of the above mentioned concepts have used basically mechanical means to tailor the aerodynamic angle-of-attack distribution. The use of aerodynamic forces to accomplish the same thing has also been employed. Kaman, in their early rotor development, used a mechanically controlled servo tab located outboard on the blade to obtain collective and cyclic pitch control. Hiller Helicopters used aerodynamic surfaces on a servo-rotor control system to control the collective and cyclic pitch angles of the main rotor. The Kaman servo-flap control system was retained in the H-43 Husky helicopter to control the blade collective and cyclic pitch angles by twisting the cantilevered blades. More recently, Kaman investigated the possible benefits of combining the servo-flap controlled blade elastic twist with blade feathering controls located at the blade root. In this configuration, the blade feathering controls were used to tilt the rotor thrust vector for trim. The blade elastic twist, controlled by the servo-flap, was used to twist the blade about its mean trim position in an attempt to provide an efficient redistribution of blade airloads to delay retreating blade stall, improve rotor performance, and reduce blade bending moments (Reference 8). The results of this investigation indicated that some stall relief was obtained and higher blade loadings could be developed without overstressing the blades. NASA has used this concept to determine if higher harmonic pitch control might provide further benefits (Reference 9).

In recent years, a number of investigations into the true use of passive aeroelastic tuning or coupling to derive beneficial results have been conducted. Gabel and Tarzanin (Reference 10) showed that, if the torsional stiffness of rotor blades was tailored such that a relatively low torsional frequency was obtained (3 to 4/rev), the oscillatory blade torsional and control loads due to dynamic stall could be reduced significantly. The torsionally soft blades, although they had only a limited effect on the stall-induced airloads forcing function, did reduce the blade response to 5/rev stall-generated aerodynamic forces, thus reducing the buildup of oscillatory loads due to a near frequency coalescence of airloads and a blade natural frequency.

8. Lemnios, Dr. A. Z., and Howes, H. E., WIND TUNNEL INVESTIGATION OF THE CONTROLLABLE TWIST ROTOR PERFORMANCE AND DYNAMIC BEHAVIOR, Kaman Aerospace Corp., USAAMRDL Technical Report 77-10, Applied Technology Laboratory, U.S. Army Research and Technology Laboratories (AVRADCOM), Ft. Eustis, Virginia, June 1977, AD A042481.
9. McCleod, John L., III, AN ANALYTICAL STUDY OF A MULTICYCLE CONTROL-LABLE TWIST ROTOR, Proceedings of the 31st Annual National Forum of the American Helicopter Society, Washington, DC, May 1975.
10. Gabel, R., and Tarzanin, F., Jr., BLADE TORSIONAL TUNING TO MANAGE LARGE AMPLITUDE CONTROL LOADS, Journal of Aircraft, Vol. II, No. 3, Paper No. 72-95, AIAA, August 1974.

The study reported by Bell in Reference 11 on the use of fore-and-aft sweep and a midspan flapping hinge to reduce control loads and midspan bending moments on wide chord blades did not really use aeroelastic couplings. However, these configurational changes did result in an alteration of the blade aerodynamic loadings and blade dynamic characteristics. The results indicated that, for the blades tested, the 1/rev control loads were not reduced by sweep, but the midspan flap hinge was very beneficial in reducing critical blade flapwise bending moments. Because of these benefits, reduced RPM operation of the rotor was obtained, which, in turn, reduced the compressibility noise generated by the blade tip. It was hypothesized in Reference 11 that if the outboard hinge had incorporated flap-pitch coupling, then the buildup of control loads with advance ratio might also be reduced significantly. Another manner of achieving this same result is through the use of aeroelastic coupling supplied by a swept-tip (Reference 12). The aeroelastic twisting provided by the swept-tip on the advancing side of the azimuth helps to reduce the destabilizing pitching moments present in this azimuth range. These destabilizing moments, generated by the drag forces acting on the blade bent downward by built-in twist, can cause torsional divergence if not controlled. As indicated in Reference 12, the aeroelastic coupling benefits of the swept-tip are not only related to benefits achievable on the advancing side, but are also realized on the retreating side in the blade stall region because of the softer blade torsional stiffness allowed by use of the blade tip sweep.

Reference 13 presents the results of an investigation in which basic blade aerodynamic parameters were used to aeroelastically control the radial and azimuthal loading distribution in an attempt to improve the rotor performance and decrease the blade oscillatory loadings. The basic parameters considered in this investigation were: reduced blade torsional stiffness, aerodynamic pitching moment (C_{M0}), outboard blade sweep, and second harmonic blade pitch control. The basic results of the exploratory program were that positive C_{M0} was beneficial as regards performance and blade dynamic bending loads. The effect of outboard blade sweep was also determined to be beneficial although it was believed that the positive effects were minimized because of an improper 2/rev phasing caused by the swept blade section.

11. Kidd, D. L., Brogdon, V. H., and White, J. A., ADVANCED TWO-BLADED ROTOR SYSTEMS AT BELL HELICOPTER TEXTRON, American Helicopter Society Mid-East Region Symposium on Rotor Technology, August 1976.
12. Arcidiacono, P., and Zincone, R., UTTAS ROTOR BLADE, Journal of the American Helicopter Society, April 1976.
13. Doman, G. S., Tarzanin, F. J., and Shaw, J. Jr., INVESTIGATION OF AEROELASTICALLY ADAPTIVE ROTORS, Boeing Vertol Co., USAAMRDL Technical Report 77-3, Applied Technology Laboratory, U.S. Army Research and Technology Laboratories (AVRADCOM), Ft. Eustis, Virginia, May 1977, AD A042083.

While the above-noted investigations touched on the use of passive aeroelastic couplings to enhance the performance and vibratory characteristics of rotor blades, they have generally been very limited in nature. This was because only one specific problem area was addressed, or because of the lack of a full understanding of all possible beneficial aeroelastic and mass-elastic couplings that can be generated by tuning modal frequencies to the frequencies of the harmonic forcing function.

This report summarizes the theoretical and experimental investigations that were conducted to evaluate the potential of aeroelastic and mass-elastic couplings to provide a truly aeroelastic conformable rotor (ACR) configuration that will improve the performance and vibratory characteristics of helicopter rotor systems without creating instabilities. The manner in which this investigation was conducted and the results that were obtained are presented in the body of this report.

PRELIMINARY INVESTIGATIONS

Selection of Primary ACR Parameters

During the initial phase of the effort, a survey of previous investigations of the effects of rotor aeroelasticity, design, and controls on the performance and operational qualities of rotor systems was conducted in order to:

1. Ensure a complete knowledge of previous efforts conducted on or closely associated with the efforts of this program.
2. Define the rotor and aircraft parameters that are significant to the aeroelastic characteristics of rotor systems.

This review included about 60 reference documents, which reported on research and engineering investigations of:

1. Higher harmonic pitch and control
2. Aeroelastic stability
3. Performance
4. Dynamic behavior
5. Control loads

References 1 through 67 are the majority of reports on the major investigations that were reviewed. In this review, the effects of the following primary categories of system parameters on rotor aeroelastic characteristics were sought to determine their relative importance:

1. Rotor aerodynamics
2. Rotor inertia
3. Blade edgewise, flapwise, and torsional stiffness
4. Blade geometry
5. Blade mass and inertia distribution
6. Blade root-end restraint
7. Blade root-to-hub orientation
8. Control system characteristics
9. Rotor-fuselage couplings
10. Mechanical couplings

On the basis of the review that was conducted, an assessment of the relative importance of various aeroelastic parameters relating to the development of

an aeroelastically conformable rotor (ACR) system was undertaken. From this evaluation, the rotor aeroelastic parameters believed to be of primary importance to an ACR system are:

1. Airfoil -- Mach number effects on aerodynamic characteristics
2. Airfoil pitching moment
3. Airfoil aerodynamic center offset from shear center
4. CG offset from shear center
5. CG offset from airfoil aerodynamic center
6. Blade planform
7. Geometric twist distribution
8. Geometric sweep distribution
9. Blade mass and inertia distribution
10. Blade torsional stiffness distribution
11. Blade edgewise stiffness distribution
12. Control system stiffness

The order in which these parameters are listed does not necessarily correspond to their order of importance. The aeroelastic parameters believed to be of secondary importance are:

1. Blade flapwise stiffness distribution
2. Pitch-flap coupling
3. Pitch-lag coupling
4. Rotor-fuselage coupling
5. Precone: predroop
6. Rotor inertia
7. Blade to blade azimuthal spacing
8. Blade to blade vertical spacing
9. Blade tip shape
10. Rotor rotational speed
11. Number of blades

The determination of whether an aeroelastic parameter is of primary or secondary importance was based on the beneficial and/or detrimental effect of the parameter in regard to improving the rotor operational qualities being considered. While the investigations reported herein primarily dealt with the parameters considered to be of primary importance, number of blades, tip shape, and blade flapwise stiffness distribution were also considered.

Selection and Description of Analysis Techniques

The various prediction capabilities that were required to successfully accomplish the theoretical analysis objectives were:

1. Prediction of aircraft trim
2. Prediction of the nonuniform wake-induced velocities
3. Prediction of the aeroelastic forced response characteristics
4. Prediction of the vibration and air and ground resonance stability characteristics

The various analyses that were evaluated for possible use in meeting these capabilities are presented in Table 1. The selection of the appropriate analytical procedures for use in this program was based on the following criteria:

1. Match of basic capabilities to requirements
2. Degree of program modifications required
3. Familiarity of technical staff with program operation
4. Availability of an IBM 360 operational version

On the basis of this evaluation, the following programs were chosen for use in the theoretical investigations conducted on this project:

1. The Rotorcraft Flight Simulation, Computer Program C81 was used for the prediction of the trim characteristics of a single-rotor helicopter having a rotor system of conventional design.
2. The Nonuniform Wake-Induced Velocity Prediction Program (NUWAIVE) was used to calculate the nonuniform wake-induced velocities for both conventional rotors and the ACR system.
3. The Rotor Aeroelastic Response Analysis (RARA) was used to predict the forced response characteristics for conventional rotors and the ACR systems.
4. The Helicopter Aeroelastic Stability Analysis (HASTA) was used to predict vibration and air resonance characteristics of the conventional and ACR systems.

A brief discussion of the capabilities of each prediction program is presented in the following paragraphs:

The C81 Rotorcraft Flight Simulation Program was chosen because it was adequate for predictions it was required to undertake, did not require any modification, and its operation was familiar to the SRL technical staff.

TABLE 1. PREDICTIVE ANALYSES EVALUATED FOR POSSIBLE USE IN PROGRAM

<u>Code</u>	<u>Developer</u>	<u>Prediction Capability</u>
C-60	Boeing Vertol	Rotor Performance, Blade Loads, and Blade Response
C81	Bell Helicopter	Helicopter Trim, Performance, Ship Stability, Blade Loads, Blade Response
G-400	UTRC	Rotor Performance, Stability Blade Loads, and Blade Response
HASTA	SRL/RASA	Helicopter Aeroelastic Stability and Blade Vibration
NUWAIVE	SRL/RASA	Deformed Free-Wake, Nonuniform Downwash Distribution
PWIA	UTRC	Rotor Inflow Based on Prescribed Wake
RAP	SRL/RASA	Rotor Acoustics
RARA	SRL/RASA	Rotor Performance, Blade Loads, and Blade Response
REXOR	Lockheed	Rotor Performance, Stability, Blade Loads, Blade Response, and Handling Qualities
NMBA	Sikorsky	Blade Loads and Blade Response
Y-71	Boeing Vertol	Rotor Vibration
6F	Kaman	Rotor Performance, Blade Loads, and Blade Response

This program has the capability of predicting the trim characteristics of a single main rotor helicopter in hover and forward flight. The mass and aerodynamic effects of the fuselage and tail rotors are included, as well as the effects of auxiliary control surfaces. In addition, a majority of the pertinent mass, elastic, and aerodynamic characteristics of conventional rotor blades are adequately represented. The details of the program capabilities are presented in Reference 14.

The C81 program was used in this effort to predict only the trim characteristics of the helicopter configuration to be studied (i.e., that helicopter is operating with rotor blades of conventional design). The program output was used to define the forces and moments on the rotor hub due to the fuselage, tail rotor, and auxiliary lifting surfaces that the main rotor must counteract in trim flight.

Nonuniform Wake-Induced Velocity Prediction Program (NUWAIVE) was chosen for use in the proposed program. It is believed to be the best available because it has been well tested and has the unique capability of predicting the wake nonuniform induced velocity field for rotors having blades of arbitrary planform for which no wake geometry data are available. In addition, the technical staff at SRL have used it extensively and know how to use it effectively.

The program in its present form can represent one rotor with up to four blades. The program can predict the free-wake positions of up to eleven discrete trailing vortex elements per blade in steady-state and maneuvering flight. The program uses as input the cyclic and collective pitch settings and the 1/rev flapping response of the blade system. All of the rotor trim input information was obtained from the output of the C81 program for the conventional rotor blades and from the RARA program for the ACR blades.

Rotor Aeroelastic Response Analysis (RARA) was chosen for use in the investigation because (1) it has all the required capabilities for investigating the aeroelastic response of ACR systems, (2) it is compatible with the HASTA stability program regarding assumptions, formulation, and required data input, (3) it has proven compatibility with the NUWAIVE analysis, (4) it has a short running time, and (5) the technical staff at SRL is very familiar with its capabilities and operation.

This predictive program is a finite-element analysis as opposed to a modal analysis and has the capability of modeling the following features of importance to ACR systems:

1. Represents the required blade characteristics of up to six blades.
2. Can be used in conjunction with the NUWAIVE free-wake analysis.

14. Davis, J. M., Bennett, R. L., and Blankenship, B. L., ROTORCRAFT FLIGHT SIMULATION WITH AEROELASTIC ROTOR AND IMPROVED AERODYNAMIC REPRESENTATION, Vol. 1 - Engineer's Manual, Bell Helicopter Co., USAAMRDL TR 74-10A, Eustis Directorate, USAAMRDL, Fort Eustis, Virginia, June 1974, AD 782854.

3. Models blades with up to 30 radial stations.
4. Uses nonlinear airfoil characteristics through the use of measured airfoil data that are a function of both angle of attack and Mach number.
5. Can adequately represent discrete offsets in shear center, center of gravity, and slopes in the blade axis system.
6. Adequately represents the various rotor articulations of interest.
7. Represents the nonuniform stiffness variations in the control system and swashplate.
8. Accounts for interharmonic couplings.

This prediction program is a descendant of the HASTA stability analysis and as such is based on identical assumptions and numerical analysis techniques as that program. While the data input is also identical to the HASTA program, the input format is different.

Helicopter Aeroelastic Stability Analysis (HASTA) was chosen for use because it is believed to be the best available, compatible with the RARA and NUWAIVE programs, and because of the familiarity of the technical staff at SRL and ATL with its use and operation. The effects of the following parameters are important to the investigation of air resonance stability problems of an ACR system which can be represented adequately by the HASTA program.

1. Nonlinear radial distribution of blade chord.
2. Nonlinear radial distribution of offsets in the edgewise location of the shear center.
3. Nonlinear radial distribution of offsets in the edgewise location of the center of gravity.
4. Stepwise variations in the sweep angle of the blade planform and shear center.
5. Nonlinear radial twist distribution.
6. Flexible control systems (cyclic and collective stiffnesses).
7. Built-in discontinuities of predroop as a function of radius.
8. The possible use of offset hinges (50 to 60 percent of radius).
9. The mean steady elastic deflections of the blade.
10. Rotor shaft flexibility or transmission rocking stiffness.
11. Fuselage mass and inertia characteristics as a free body.
12. Landing gear stiffness characteristics.

Selection of Operational Qualities to be Improved

The major operational qualities that were considered for investigation were the following:

1. Rotor propulsive efficiency
2. Rotor vibratory loads in the rotating field
3. Transmitted vibration to the fixed or fuselage system
4. Overall rotor performance
5. Blade stresses
6. Aircraft handling qualities (control power)
7. Rotor acoustics
8. Rotor and blade stability

It was believed that the first five qualities listed are of primary importance and, if improved, might provide the greatest potential for improving the capabilities of present-day and advanced helicopters. While rotor hovering efficiency is of great importance, it was felt that desired improvements could be obtained by the appropriate use of blade design parameters and that the utilization of aeroelastic effects is not necessarily required.

Handling qualities (control power) was also believed to be a parameter of somewhat secondary importance to the present study in that parameters other than aeroelastic couplings usually can be used to provide adequate control power. Since handling qualities are somewhat dependent rather than independent parameters, the effects of aeroelastic couplings on these qualities were investigated separately.

Rotor acoustics was also considered to be a dependent rotor quality in the investigation, as was rotor blade stability and, therefore, neither of these parameters were investigated.

On the basis of engineering judgement and the above reasoning, the primary operational qualities 1 through 5 above were investigated in the program.

Selection of Basic Rotor Configuration

It was believed that the improvement in rotor operational qualities due to ACR would be basically the same for all types of rotor systems and, therefore, the qualities selected for investigation did not have a major influence on the selection of the rotor system to be analyzed. The basic

types of rotor systems that were considered as candidates for an ACR system are:

<u>System Type</u>	<u>Number of Blades</u>
Teetering	2
Fully Articulated	3 to 6
Hingeless	3 to 6
Bearingless	2 to 6

During the ACR rotor system selection process, the following factors were considered:

1. The rotor system most representative of current Army aircraft under development.
2. The rotor system that will provide the most flexibility in varying parameters during the test phase.
3. The rotor system for which the basic parameters can be well defined.
4. The rotor system that will provide the best possibility of being analyzed for stability problems and for which "unknown" stability parameters are probably not present.
5. The most general applicability of the results that can be obtained.

On the basis of these considerations, the fully articulated rotor system having four blades was selected for analysis, construction, and test. It was believed that this rotor configuration rates the highest of the above-noted rotor systems for the following reasons:

1. A four-bladed system is the one in most general use today and is being used in the development of the new generation of Army operational helicopters.
2. The articulated rotor system is being used in the new generation of operational Army helicopters.
3. The articulated rotor system has the capability for permitting well-defined changes in δ_3 , δ_2 , offset axes, and other parameters.
4. It is the rotor system that has better defined and predictable stability characteristics when conventional blades are being used.

The baseline rotor system for which the investigations of the ACR concept were conducted was a 9-foot-diameter, four-bladed, fully articulated model with a constant chord and 8 degrees of linear twist. The mass and elastic properties of the blades had typical distributions with mean values such that Mach, Froude, and Locke scaling from a full-scale blade were correct when the model was tested in the NASA Transonic Dynamics Tunnel in a Freon 12 environment.

THEORETICAL INVESTIGATION OF ACR CONCEPT

Description of the Computational Procedure

The ACR blade concept was investigated by altering the basic characteristics of the baseline blade. The primary parameters of the baseline blade that were altered during the investigation were:

Geometric

1. Radial distribution of planform
2. Radial distribution of twist
3. Hinge pitch-flap coupling
4. Hinge flap-lag coupling
5. Radial distribution of sweep

Stiffness

1. Radial distribution of flapwise stiffness
2. Radial distribution of edgewise stiffness
3. Radial distribution of torsional stiffness
4. Control system stiffness
5. Offset of shear center

Mass

1. Radial distribution of torsional inertia
2. Radial distribution of mass
3. Radial distribution of center of gravity
4. Concentrated masses to tune or detune modal couplings through mode shape control

The geometric and drag characteristics of the S-61 helicopter having a weight of approximately 14,000 pounds was the basic aircraft configuration modeled for use in the studies reported herein. While the geometric characteristics of the four-bladed, articulated S-61 rotor were also used in the analytical studies, the airfoil section, mass and twist distributions of the rotor blades did not correspond to the S-61 helicopter. The basic reason for using a scaled version of the S-61 helicopter as the flight vehicle was its compatibility with the model rotor hub of the ARES test system in the NASA Transonic Dynamics Tunnel. In addition, data obtained previously with scaled S-61 blades on the ARES model could be used to establish load limits for the model system.

The C81 analysis was used initially to establish the rotor hub forces and moments that the rotor must develop to trim the aircraft over a range of advance ratios and loading conditions. For the assumed nominal single-rotor helicopter used in these studies, the analysis was used to compute the shaft trim loads over an advance ratio range of $\mu = 0$ to 0.45 for a 1 g loading condition. Computations were made for each advance ratio at increasing load conditions until the rotor could no longer develop the required forces and moments to trim the aircraft. These were then the "standard" forces and moments that the rotor system, either the baseline or the ACR rotor, must match to trim the assumed helicopter configuration. The above-noted use of C81 to determine the shaft loads required to trim the aircraft over a range of advance ratios and loading conditions was the only time the program was used during the subject investigations.

For a given loading condition, the collective pitch, cyclic pitch, coning, and 1/rev flapwise response determined by use of the C81 analysis was used as input to the NUWAIVE program to compute the velocity field induced by the free rotor wake. These induced velocities were then input to the RARA analysis to predict the shaft loads generated by the rotor. If the specified shaft trim loads were not obtained using the RARA analysis, the collective and cyclic pitch angles were perturbed to obtain estimates of new control settings for force and moment trim. Once trim had been achieved by this procedure, the zero and first harmonic flapwise, edgewise, and torsional deflections of the rotor blades were determined. These deflections were then compared with those originally used as input to the NUWAIVE program. If there were significant differences of these various deflections, the updated deflections computed by RARA would be used in NUWAIVE to compute a new set of induced velocities to be used in RARA to compute a new set of shaft loads. This procedure would be repeated until the "required" shaft trim loads were obtained and there was consistency between the collective and cyclic pitch angles (including elastic twist), the coning and 1/rev flap angles used in NUWAIVE and RARA. The results obtained by this procedure for the baseline blades and the various ACR concepts were compared on the basis of C_T/C_0 to evaluate the effectiveness of the ACR design parameters in improving the rotor performance characteristics as a function of advance ratio and loading.

It was noticed, that the predicted performance characteristics improved significantly with the replacement of the uniform wake with the first estimate of the nonuniform wake-induced velocities, based on the control parameters predicted by C81. It was also noted that, as might be expected with the more flexible ACR concepts, the interaction of the wake and blade elastic deformations were much more pronounced as the maximum loading of the rotor system was approached.

The HASTA analysis was used to compute the air resonance modes of both the baseline blades and the final ACR blade design chosen for construction.

Results of the ACR Concept Studies

Using the calculation procedures outlined in the previous section, the effects of various blade parameters on the performance characteristics of the baseline blade were investigated to determine the best combination of parameters to enhance the rotor performance in terms of the ACR concept. While the analyses were conducted over a range of advance ratios and loading conditions, the majority of analyses were conducted at an advance ratio of $u = 0.35$ at a loading condition near the limit of the rotor system. An initial investigation was conducted with a blade having a torsional stiffness 1/3 of that of the baseline blade, to determine the effect of built-in twist on the rotor performance characteristics. The results of the investigations conducted for -8, -12, and -14 degrees of built-in twist indicated that -8 degrees was probably the better value of twist; therefore, all following calculations were conducted with that value.

The range of parameters that were varied to evaluate their effect are as follows:

Aerodynamic Center:	0.25C, 0.30C, and 0.35C from 60 to 80 percent R
Shear Center:	0.25C and 0.40C from 60 to 80 percent R
Center of Gravity at 60 percent Span:	0.25C and 0.10C by the addition of weight
Swept Tip:	20 degrees sweep at 92 percent R; 20 degree sweep at 82 percent R
Blade Taper:	1.35/1
Blade Torsional Stiffness:	(1) 1/3 of baseline blade from 0 to 100 percent R (2) 1/6 of baseline blade from 0 to 100 percent R (3) 1/6 of baseline blade from 0 to 50 percent R and 1/12 of baseline blade from 50 to 100 percent R

The comparative performance benefits obtained by the use of the parameter variations noted above are presented in Table 2.

The results presented in this table indicate that reducing the torsional stiffness of the baseline blade by six times and adding 20 degrees of tip sweep at 82 percent R provided the largest performance benefit. While the results imply that adding the swept tip to a blade having a six times

torsional stiffness reduction from 0 to 50 percent R and a 12 times reduction from 50 percent R to 100 percent R might have a larger performance gain, difficulties in blade construction ruled out further consideration of this configuration.

TABLE 2. RELATIVE PERFORMANCE BENEFITS OF ACR PARAMETERS*

	Rectangular Tip	Swept Tip 82° R	CG Location	AC Location	Shear Center Loc.	Blade Taper
Baseline Blade Stiffness	-	-	-	1*	-	-
Torsional Stiffness, 1/3 Baseline	1	-	-	2	2	-
Torsional Stiffness, 1/6 Baseline	7.5	10	6.9	-	-	5.0
Torsional Stiffness, 1/6 Baseline IB 1/12 Outboard	8	-	8	-	-	-

*Numbers are percent of performance (T/Q increase over baseline blade times 10 divided by maximum increase that was calculated.

On the basis of the results presented, it was concluded that the ACR blade would be based on reducing the torsional stiffness of the baseline blade by a factor of six and adding 20 degrees of tip sweep from 92 to 100 percent of blade radius.

The HASTA analysis was applied to the ACR blade design (a torsionally softer blade with swept tip) and the baseline blade design to determine the suitability of these designs in regard to their frequency and stability characteristics.

The natural frequency results for the baseline blade design at the high thrust $\mu = 0.35$ advance ratio condition are shown in Figure 1. The only area of concern at or near the operational RPM was the proximity of the third flap frequency to the 5/rev multiple of the rotor RPM. The natural frequency results for the ACR blade design for the same operating conditions are shown in Figure 2. At or near the nominal operating RPM there were three possible areas of concern in regard to the ACR blade design characteristics. These are the proximity of the first torsion mode and the 4/rev

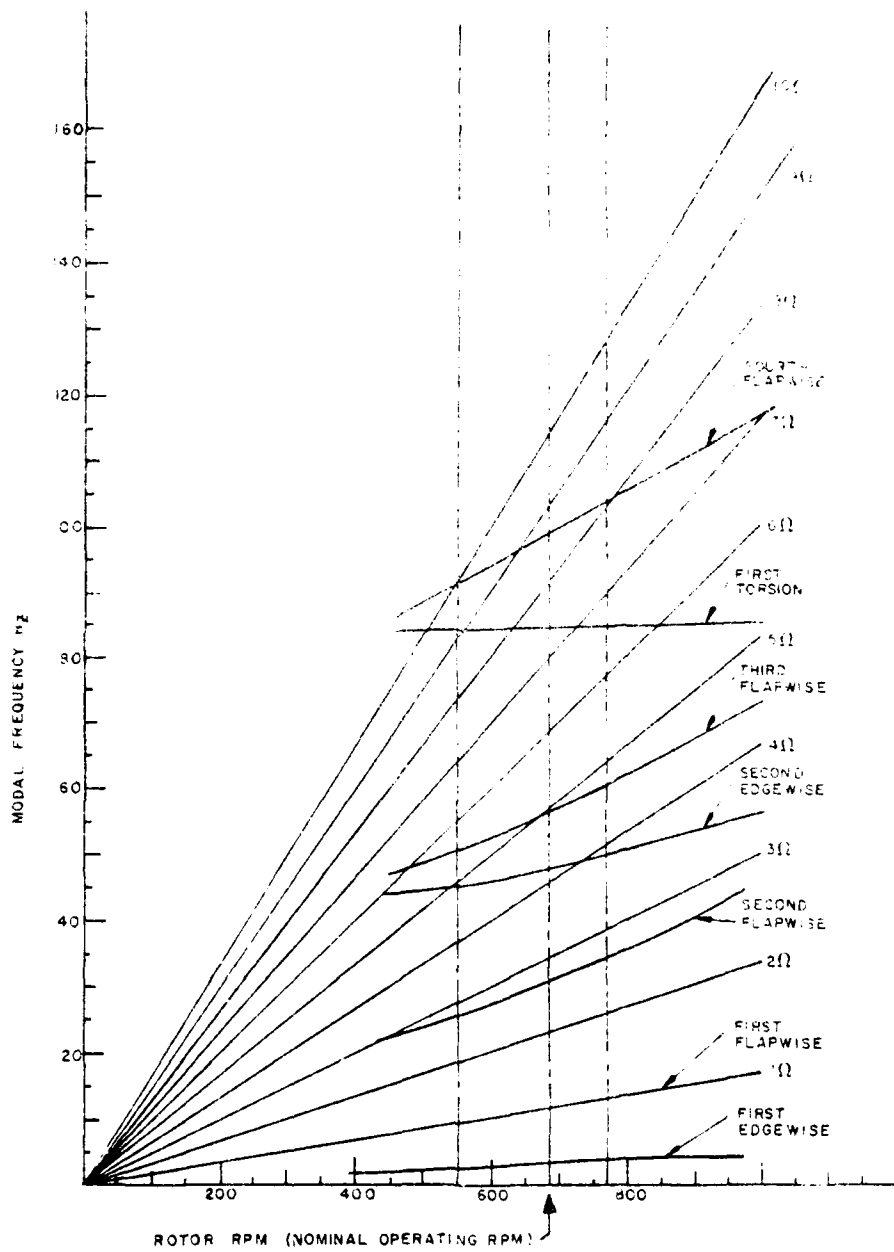


Figure 1. Modal Frequency vs. Rotor RPM for Baseline Blade.

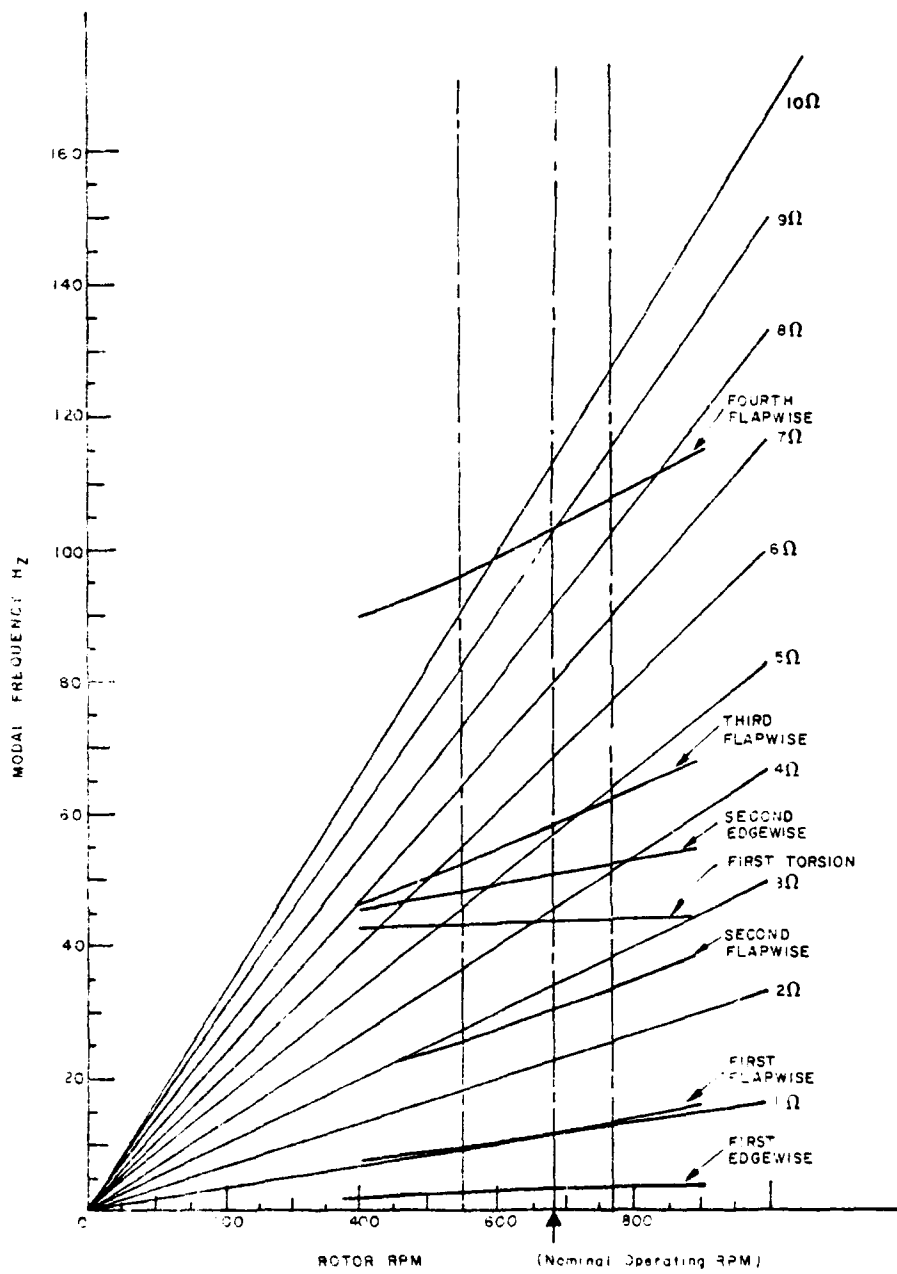


Figure 2. Modal Frequency vs. Rotor RPM for ACR Swept-Tip Blade.

rotor RPM multiple, the third flap mode and the 5/rev rotor RPM multiple, and the fourth flap mode and the 9/rev rotor RPM multiple.

Based on the HASTA predicted stability characteristics, both the baseline and the ACR blade designs are significantly damped for the high thrust 0.35 advance ratio operating condition. The degree of damping predicted for the various modes is given in Table 3 in terms of the time required for an oscillation to be damped to one-half amplitude.

TABLE 3. DEGREE OF DAMPING PREDICTED FOR VARIOUS MODES

<u>Model Type</u>	<u>Half Amplitude Time, sec</u>	
	<u>Baseline Design</u>	<u>ACR Design</u>
1st Edgewise	0.469	0.495
2nd Edgewise	0.0652	0.0481
1st Flapwise	0.0424	0.0368
2nd Flapwise	0.0549	0.0480
3rd Flapwise	0.0718	0.0434
4th Flapwise	0.0466	0.0294
1st Torsion	0.0109	0.0070

The above values were obtained assuming a reactionless type of mode without blade structural damping effects being included. Stability results predicted for umbrella, backward cyclic, and forward cyclic types of modes, with inclusion of a control system representative of that of the existing test stand, were essentially unchanged from those predicted for the reactionless modes except for the first torsion mode. This was even more damped than for the other mode types.

BLADE CONSTRUCTION

General Design Factors

The definition of the basic model rotor system required the specification of full-scale system parameters such as rotor RPM and thrust. Thus, four-bladed rotor system characteristics of a rotor radius of 24 feet (288 inches), a rotor rotational speed of 289 RPM, and a nominal thrust of 13,825 pounds were chosen for the full-scale rotor system. These full-scale rotor system values are representative of a rotor system that could be used on a helicopter such as the YAH-64. With the linear dimension scaling factor for converting from full-scale dimensions to scale model dimensions defined by the ratio of model blade radius to full-scale blade radius ($55/288$ or 0.0191) and the Freon 12 to airspeed of sound and density ratios defined as $505/1116$ (0.4525) and 3.0 , respectively, scale factors for other system parameters were defined. The scale factors for some of the more important rotor system parameters are provided in Table 4. The coefficient of viscosity scale factor of 0.0705 was also used. Consistent with scale factors presented in Table 4 and the various chosen model and full-scale parameters, the characteristics of the baseline scale model rotor system and the full-scale rotor system it represents are summarized in Table 5.

The original intent of the rotor design was to have the baseline model correspond to that required for use in a Freon 12 environment with a density of 0.009512 slugs/ft³. The final model corresponded to that required for testing at a density of 0.007134 slugs/ft³ (three times air atmosphere density). This density reduction was necessary in that simultaneous satisfaction of the higher blade mass and stiffness-related parameter values required in the physical model for the higher density environment would be difficult, if not impossible, within the confines of the blade thickness and chordwise dimensions. Further, the Freon 12 fill and purge cycle time required in the Transonic Dynamics Tunnel for the higher density would restrict the amount of data that could be obtained within the allocated tunnel time. Specifically, the baseline blade design has a span of 55 inches from rotor hub centerline to blade tip. The airfoil portion of the blade, which begins at 12.5 inches from the hub centerline, is a NACA 23012 airfoil having a chord length of 4.24 inches. The blades include a built-in linear twist from the 9-inch spanwise station ($R = 9$ inches) to the blade tip, which corresponds to a leading-edge-down twist of 8 degrees over the full blade span. The design spanwise distributions of the mass and elastic properties of the blades are depicted in Figures 3 through 8. The values of these parameters measured on the model blades are given in Table 6. Tables 4, 5, and 6 follow on the next pages, as do Figures 3 through 8.

TABLE 4. SUMMARY OF ROTOR SYSTEM CHARACTERISTICS FOR THE ANALYTICAL SCALE MODEL AND FULL-SCALE ROTOR SYSTEM

<u>Description</u>	<u>Scale Model</u>	<u>Full-Scale</u>
Rotor Type	Fully Articulated	Fully Articulated
Number of Blades	4	4
Rotor Diameter	110 in.	40 ft
Blade Chord	4.24 in.	22.2 in.
Solidity	0.0982	0.0982
Blade Twist	8°	8°
Root Cutout	12.5 in.	5.456 ft
Airfoil Section	NACA 23012	NACA 23012
Hinge Offsets	3.0 in.	1.309 ft
Blade pitch axis	25% Chord	25% Chord
Blade Shear Center	25% Chord*	25% Chord*
Blade CG	0.001 in. Aft of Shear Center	0.052 in. Aft of Shear Center
Lead-Lag Stiffness	460 in.-lb/rad	8960 ft-lb/rad
Lead-Lag Damping	22.91 in.-lb-sec/rad	1057 ft-lb-sec/rad
Blade Flapping Mass	0.03136 lb-sec/in.	12.21 slugs
Blade First Moment of Inertia	0.4416 lb-sec	110.7 slug-ft
Blade Second Moment of Inertia	14.612 lb-sec-in.	1598.0 slug-ft ²

* Values are those over the uniform portion of the blade

TABLE 5. SYSTEM PARAMETER SCALE FACTORS FOR THE BASELINE MODEL DESIGNED FOR TESTING IN FREON 12

<u>Parameter</u>	<u>Scale Factor</u>
Speed of Sound	0.4525
Coefficient of Viscosity	0.705
Density	3.0
Length	0.1910
Mass	0.0209
Bending Stiffness	0.000817
Tip Speed	0.4525
Velocity	0.4525
Mach	1.0
Advance Ratio	1.0
Angular Velocity	2.3695
Froude Number	1.0722
Reynolds Number	0.3677
Locke Number	1.0
Structural Frequencies	2.3695
Per Rev Structural Frequencies	1.0
Thrust Coefficient	1.0
Rotor Solidity	1.0

TABLE 6. WAS. ELA. I.C. PROPERTY. 1. 1950. 1. 1950. 1. 1950. 1. 1950. 1. 1950.

Station	Mass/Unit Length		Torsional Properties		Effect of Gravity Offset	
	Baseline lbs/in.	ACR lbs/in.	Baseline lb-sec x 10 ³	ACR lb-sec x 10 ³	Baseline in.	ACR in.
55.00-54.61	0.0310	0.0314	0.6094	0.6094	0.104	-0.068
54.61-53.51	0.0534	0.0598	0.7270	0.7380	-0.067	-0.067
53.41-51.86	0.0558	0.0620	0.8802	0.8916	-0.067	-0.067
51.86-48.96	0.0725	0.0786	1.1209	1.1980	-0.106	-0.168
48.96-46.86	0.1105	0.1130	1.7890	1.7850	+0.04	+0.052
46.86-43.37	0.1085	0.1107	1.8732	1.8250	0.04	0.052
43.37-40.45	0.1562	0.1600	2.6280	2.6249	0.04	0.052
40.45-39.57	0.1156	0.1195	2.1020	2.1090	0.04	0.052
39.57-36.65	0.1037	0.1067	1.6530	1.6500	0.04	0.052
36.65-34.73	0.1165	0.1195	2.0670	2.0640	0.04	0.052
34.73-31.81	0.1135	0.1163	1.9600	1.9570	0.04	0.052
31.81-29.63	0.1164	0.1194	1.9590	1.9580	0.04	0.052
29.63-26.70	0.1165	0.1193	1.9600	1.9570	0.04	0.052
26.70-24.53	0.1052	0.1063	1.8800	1.8780	0.04	0.052
24.53-20.32	0.1100	1.1139	1.7210	2.0050	0.04	0.052
20.32-17.56	0.1140	0.1206	2.0670	2.0630	0.04	0.052
17.56-13.55	0.1225	0.1248	1.9420	1.9390	0.040	0.052
13.55-11.38	0.0886	0.0774	0.8610	0.8595	0.048	0.055
11.38- 6.58	0.1128	0.1083	0.4700	0.9394	-0.101	-0.104
6.58- 4.40	0.2356	0.2353	3.1520	3.1480	0.0	0.0
4.40- 0.00	0.2138	0.2135	2.8100	2.8060	0.0	0.0

TABLE 6. MASS ELASTIC PROPERTIES OF BASELINE AND ACR BLADES - continued

Station	Torsional Stiffness		Flapwise Stiffness		Edgewise Stiffness	
	Baseline lb-in ² x 10 ⁻⁵	ACR lb-in ² x 10 ⁻⁵	Baseline lb-in ² x 10 ⁻⁵	ACR lb-in ² x 10 ⁻⁵	Baseline lb-in ² x 10 ⁻⁶	ACR lb-in ² x 10 ⁻⁶
55.00-54.61	0.00	0.00	0.00	0.00	0.00	0.00
54.61-53.51	0.3504	0.3504	0.3632	0.3632	0.7963	0.7963
53.51-51.86	0.3580	0.3580	0.3680	0.3680	1.0780	1.0780
51.86-48.96	0.3578	0.3578	0.3678	0.3678	1.0660	1.0660
48.96-46.86	0.4386	0.1818	0.4638	0.5551	0.7978	0.8562
46.86-43.37	0.4920	0.1300	0.4670	0.4840	0.8920	0.9100
43.37-40.45	0.4920	0.1300	0.4670	0.4840	0.8920	0.9100
40.45-39.57	0.4920	0.1300	0.4670	0.4840	0.8920	0.9100
39.57-36.65	0.4920	0.1300	0.4670	0.4840	0.8920	0.9100
36.65-34.73	0.4920	0.1300	0.4670	0.4840	0.8920	0.9100
34.73-31.81	0.4920	0.1300	0.4670	0.4840	0.8920	0.9100
31.81-29.63	0.4920	0.1300	0.4670	0.4840	0.8920	0.9100
29.63-26.70	0.4920	0.1300	0.4670	0.4840	0.8920	0.9100
26.70-24.53	0.4920	0.1300	0.4670	0.4840	0.8920	0.9100
24.53-20.32	0.4920	0.1300	0.4670	0.4840	0.8920	0.9100
20.32-17.56	0.4920	0.1300	0.4670	0.4840	0.8920	0.9100
17.56-13.55	0.4920	0.1300	0.4670	0.4840	0.8920	0.9100
13.55-11.38	0.4920	0.1300	0.4670	0.4840	0.8920	0.9100
11.38- 6.58	0.4370	0.8395	0.4226	0.4818	0.6282	0.6713
6.53-4.40	10.0000	10.0000	50.0000	50.0000	50.0000	50.0000
4.40-0.0	10.0000	10.0000	50.0000	50.0000	50.0000	50.0000

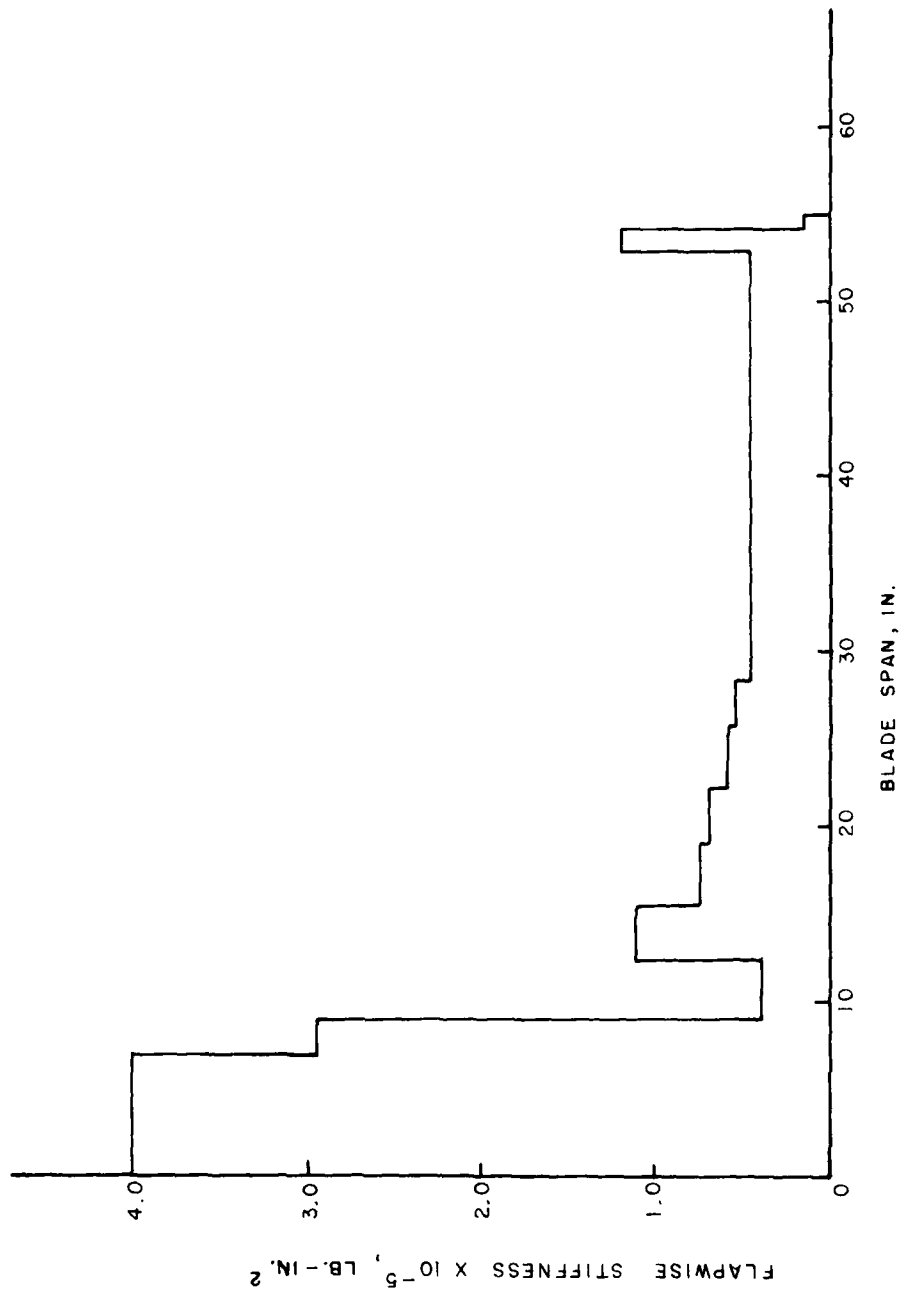


Figure 3. Baseline Blade Analytical Model Flapwise Stiffness Distribution.

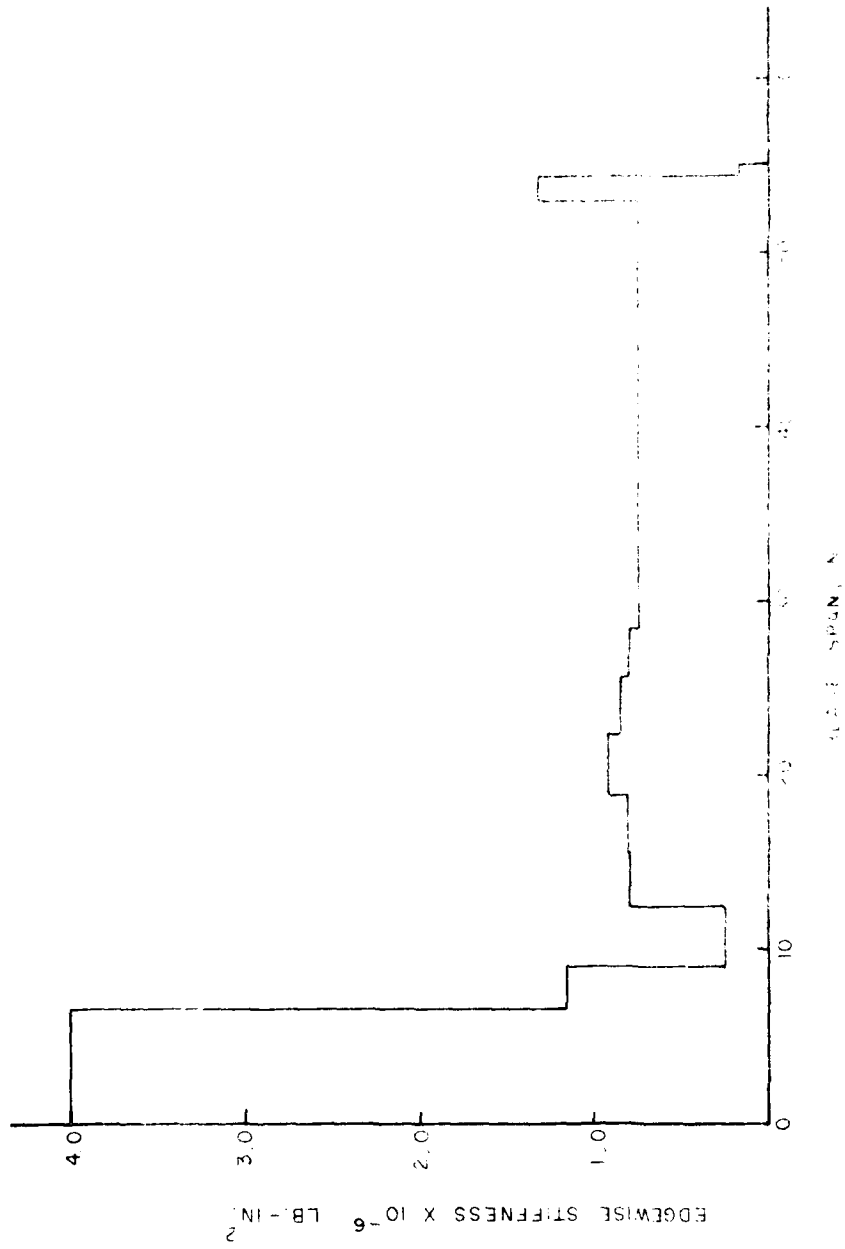


Figure 4. Baseline Data for the 100' Span Bridge.

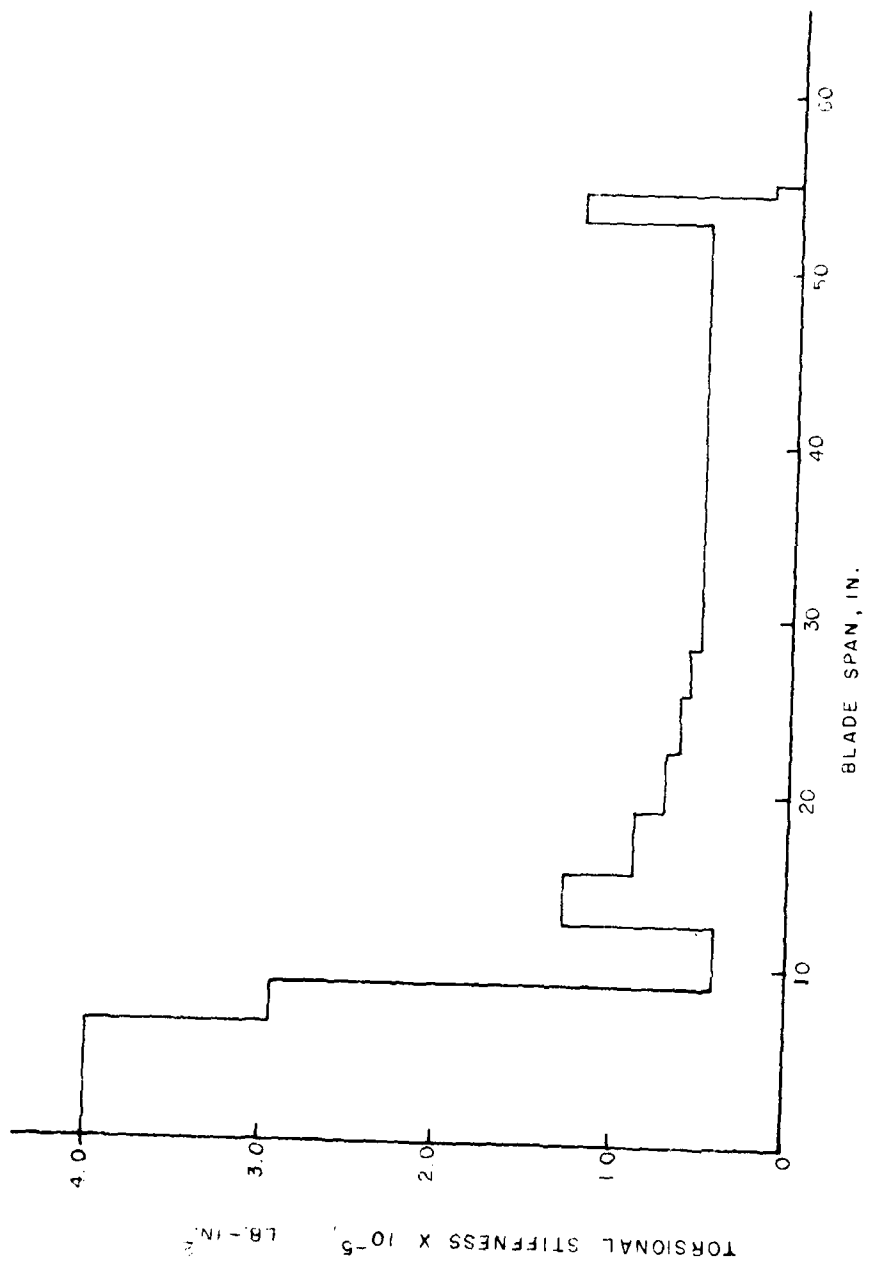


Figure 5. Baseline Blade Analytical Model Torsional Stiffness Distribution.

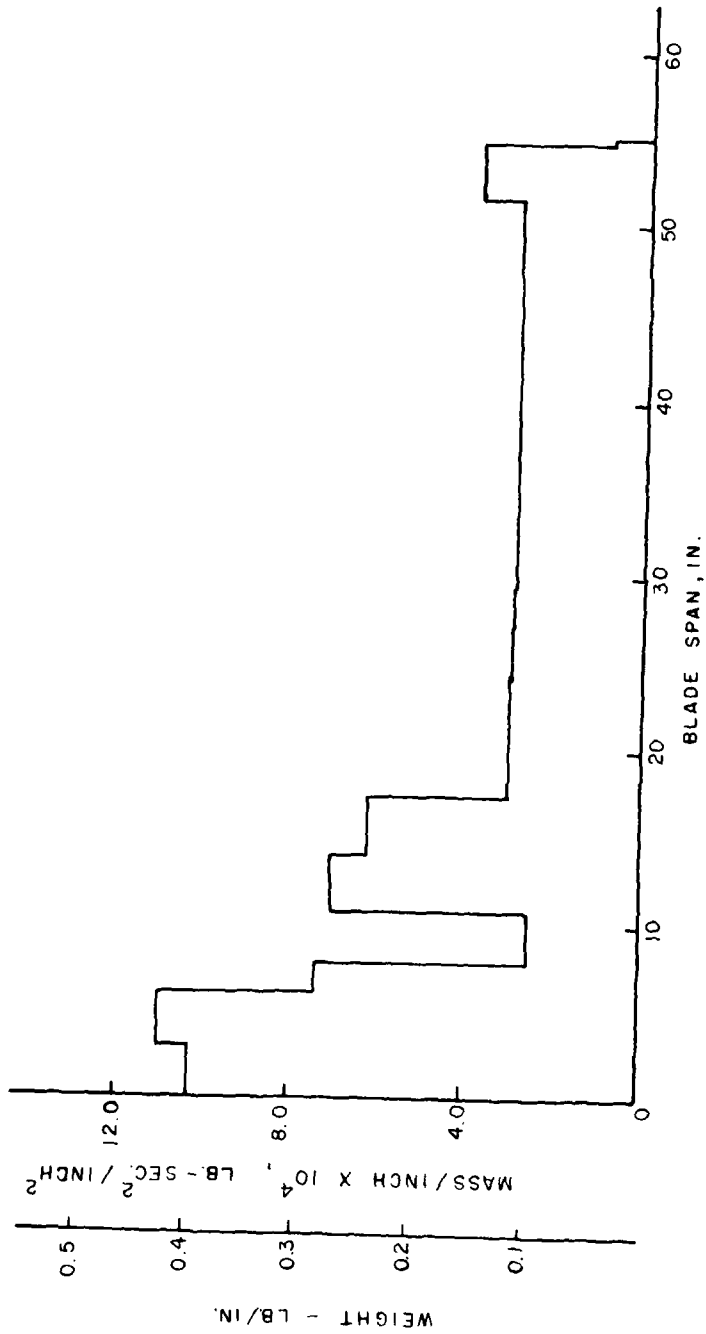


Figure 6. Baseline Blade Analytical Model Mass and Weight per Inch Distribution.

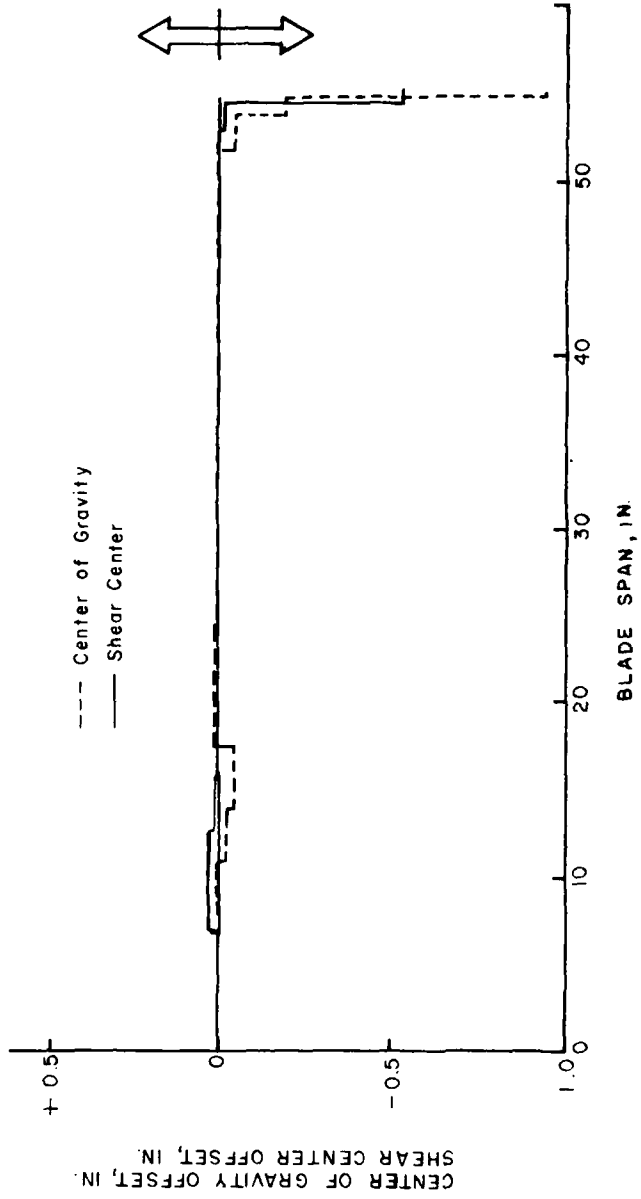


Figure 7. Distributions of Baseline Blade Analytical Model Center of Gravity and Shear Center Axis Offsets Relative to Blade Pitch Axis (at 25% Chord).

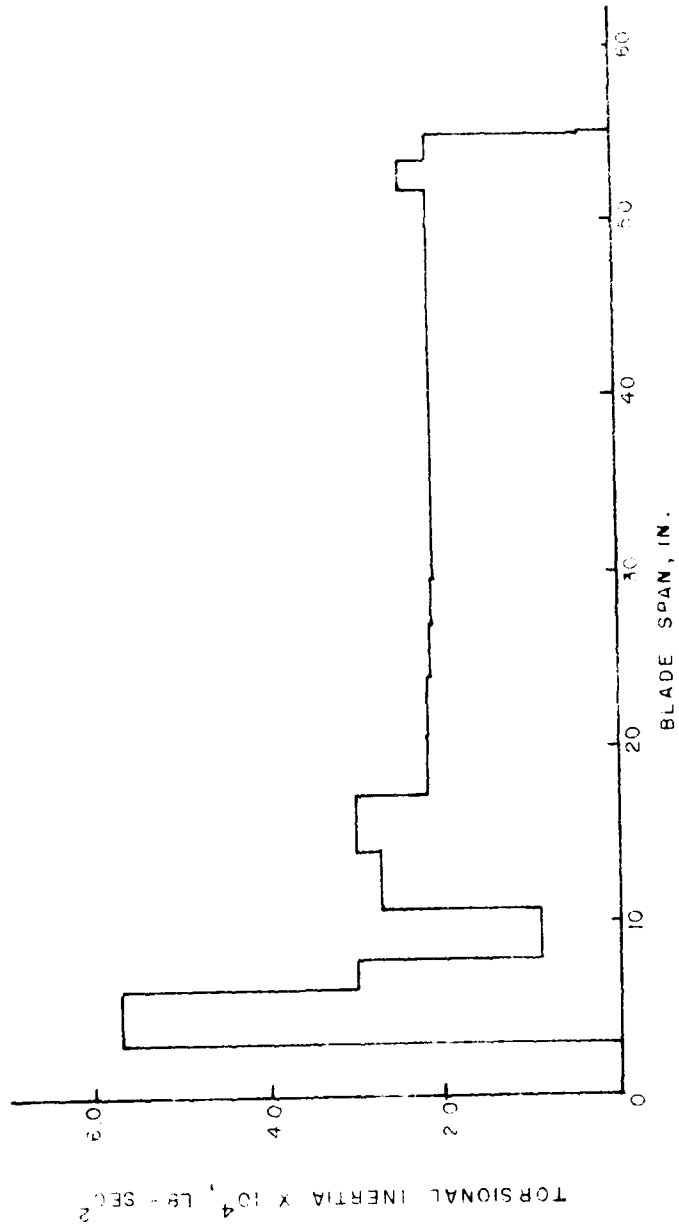


Figure 5. Baseline Blade Analytical Model Torsional Inertia Distribution.

The ACR blade rotor system was chosen to be identical to the baseline model except for parameter changes associated with the reduction in blade torsional stiffness by a factor of six in the airfoil portion of the blade (R = 12.5 in. to 55 in.) and the inclusion of a swept tip. (Note: A reduction factor of approximately four was actually used. The values of the pertinent mass and elastic parameters measured for the ACR model blades are presented in Table 6.) These blade modifications, based on the extensive theoretical investigation presented elsewhere in this report, provided the greatest predicted improvement in rotor system performance characteristics of the various modifications considered. The swept tip design corresponds to the curboard 8 percent of the blade span being swept back 20 degrees aft from the blade pitch axis (the 8 percent chord without an incremental pitch change occurring at the interface of the blade and tip. The section chord length of the swept tip chord in the direction perpendicular to the swept tip spanwise axis is the same as that of the rest of the blade (4.24 in.). In designing the swept tip, the spanwise length was defined so that the rotor radius for the ACR blade system is identical to that of the baseline. To maintain the same blade tip built-in twist value for the two blade models, the swept tip twist per unit length was reduced accordingly.

The physical realization of both the baseline and ACR analytical model rotor blades was undertaken based upon a proven model rotor system design philosophy. The specific approach taken was to provide the majority of flapwise, edgewise, and torsional stiffness characteristics in the blade spar only. This concentration of mechanical qualities in the spar allows adjustment through easily controlled machining procedures for either a composite spar mold or a metallic spar. The determination was made early in the program to use a homogeneous metal blade spar, if possible, to minimize subsequent manufacturing cost, i.e., additional patterns, molds, and composite layups.

The last major design criterion concerned achieving maximum repeatability in the manufacturing process to preclude both rotor system balance and tracking difficulties. This is especially important for model rotor blades used on the NASA/Langley ARES system which requires a complete pump down and recharge cycle to enter the tunnel for each tracking adjustment made in Freon. To satisfy this criterion, the baseline and ACR blades were designed so that all final test units were manufactured using a common set of semi-permanent non-steel tools.

With the decision made early in the design process to use a homogeneous metallic main blade spar that would provide the major portion of the desired mechanical characteristics, a trade-off analysis was undertaken of candidate materials. These materials included aluminum, carbon steel, and the more exotic stainless steels.

The investigation into materials revealed that an aluminum spar would present severe difficulties in meeting the mass characteristics required by the three times atmospheric test media density. It was found that the

ballasting of the rotor blades would become the primary mechanical factor rather than the aluminum spar. Composite material spars such as epoxy/fiberglass or graphite/epoxy were also eliminated due to the ballast weighting problems and tooling costs. Therefore, the trade-off study was concentrated on more dense materials that would also meet the mechanical requirements.

The entire range of steels was examined, from the common variety, e.g., 1020, to the high-strength aircraft-quality heat-treatable class, e.g., 4340. Lower-strength materials were eliminated because of the stress requirements of the ACR spar design's small cross-sectional areas.

The high-strength steels were also eliminated because of the machining requirements of long cuts on small cross-sectional areas; these cuts are extremely difficult to control dimensionally without the high added expense of special tooling. Also, there was a concern that the mechanical characteristics (stiffness) might be degraded over a period of time because of the vibratory loadings on the spars.

Another consideration in the elimination of the aircraft carbon steels was the need to heat treat these materials to the required strength level before machining (adding cost due to the loss in machinability) or after machining (resulting in dimensional changes and requirements for subsequent secondary finish operations).

Based on these factors, other candidate materials that could provide high strength, relative ease of fabrication, and dimensional stability were reviewed. Because the ACR requirements closely follow those of model balance systems and flexures for stability studies with which SRL has had extensive experience, the 17-4 PH* stainless steel used in the hardware for those programs was investigated in depth. 17-4 PH is a precipitation-hardening stainless steel that has a combination of high strength and hardness, excellent corrosion resistance, and is easily heat treatable. Additional features of the material, important when considering its use for the spars, are its high resistance to crack propagation, good transverse properties, and proven resistance to stress corrosion cracking. 17-4 PH is magnetic in its heat-treated form, which results in an added machining advantage due to less complex fixturing; i.e., magnetic chucks such as on a surface grinder can be used. The ease of heat treating this material and its dimensional stability (less than 2 percent shrinkage), combined with excellent machinability in the HH1150 condition, further confirmed the desirability of its selection. Table 7 provides a listing of the mechanical properties of 17-4 PH stainless steel.

* 17-4 PH is a registered trademark of Armco Steel Corp., Middletown, Ohio.

TABLE 7. 17-4 PH (H1150) STAINLESS STEEL MECHANICAL PROPERTIES

Property	SOURCE	
	ARMCO ^a	REFERENCE ^{*b}
Ultimate Tensile Stress, KSI	145, 135	134, 125
Tensile Yield Stress, KSI	125, 105	115, 100
Ultimate Shear Stress, KSI ^c		
Torsion	124	
Double Shear	90.84 ^d	
Shear Yield Stress in Torsion, KSI	42.5	Not provided
Fatigue Strength, KSI		
10 million cycles	90	
100 million cycles	90	

- Notes:
- a. When two numbers are provided in this column, the first is a typical value and the second is the minimum value.
 - b. When two numbers are provided in this column, the first value is that which at least 90 percent of the material samples will equal or exceed with a confidence level of 95 percent and the second value is that which at least 99 percent of the material samples will equal or exceed with a confidence level of 95 percent.
 - c. Values represent the average shearing stress over the cross section but the method of determination is not known.
 - d. Values presented based on 62 percent of the ultimate tensile stress rather than 68 percent to be more consistent with test results obtained for this material with other heat treatments.

*Military Handbook, MIL-HDBK-56, Metallic Materials and Elements for Aerospace Vehicle Structures, Department of Defense, Washington, D.C., 15 September 1976.

The selection of the spar as the primary mechanical unit of the model rotor blade system structure brought forth the second area of concern in the design process. This concern was the selection of materials for the airfoil and skin components so that their combined mechanical influence on the system was minimized.

This approach has been standard operating procedure for aerodynamic flutter models for years, where airfoil sections are primarily nonstructural. The materials selected for the ACR program consisted of a 2-lb/ft³ polyurethane foam core (both preformed and foamed in place) covered by an epoxy/fiber-glass skin. Although this basic concept was closely followed during the design process, some modification to the trailing edge due to mass moment considerations was required in the final test articles, as outlined later.

The specific design, fabrication, and mechanical acceptance testing procedures successfully undertaken for the baseline and the ACR model blade sets are presented in the following sections.

Baseline Blade Design

A design procedure using both the analytical representation values and experimental test results was completed in an iterative fashion to arrive at the final design of the baseline blades. This design was based specifically upon the mass and stiffness properties of the uniform spanwise portion of the analytical model.

The general procedure related to the design iteration that was conducted is presented below:

1. Calculate the specific spar dimensions and relative position with respect to the 25 percent chord line, based on analytical properties.
2. Design a twenty-four-inch-span test sample of the complete blade section, using the calculated dimensions.

(Note: The test samples were required because of the unknown properties resulting from the nonstructural laid-up composition of the airfoil section. Characteristics such as the spanwise (EI) and torsional (GJ) stiffness values could not be conclusively established by calculation.)

3. Statically test the sample employing a specially designed set of test fixtures that use calibrated weights traceable to the National Bureau of Standards (NBS).
4. Calculate the actual sample properties from the test results.
5. Recalculate dimensions and revise the design, if required.

6. Construct new or modify existing test samples.
7. Retest to confirm the revised design.

The resulting baseline blade design is shown in Figure 9. The specific design details of the blade shown include: the 17-4 PH (H1150) stainless steel rectangular spar, the cast epoxy trailing edge, the ballast weights, the two-part polyurethane core, the laidup fiberglass skin, and the two interchangeable blade tips.

Further discussion of the baseline blade system design is provided in the Blade Fabrication Section.

ACR Blade Design

The ACR blade design procedure was essentially the same general approach as that for the baseline with the exception of the dimensions of the spar. The ACR blade final assembly is shown in Figure 10.

As outlined earlier, the primary feature of the ACR design, which evolved during the analysis phase, was a reduction in blade torsional stiffness by a factor of six. An H-shaped spar cross section was adopted, which permitted a reduction in torsional stiffness while the flapwise stiffness matched that of the baseline blade. The spar cross section that resulted from this approach barely fit within the airfoil contour which led to a problem that could not be solved in the context of the model rotor system design philosophy. The proximity of the spar to the skin resulted in an unexpectedly strong bond between them. This provided a very effective torque box in the aft portion of the blade and limited the stiffness reduction to a factor of approximately four. For the simple static case this implies that a given twisting moment would produce only two-thirds the torsional deflection that was originally hoped for. This is borne out in the test data, which show ACR benefits only at the higher thrust levels.

The actual design of the ACR blade closely followed the baseline effort; the same iterative procedure was used. Sample blade sections were constructed, tested, and the design revised until the final configuration was determined.

Further details of the ACR design are outlined in the Blade Fabrication Section.

Stress Analysis

In conjunction with the design of both the baseline and ACR model rotor blade systems, a structural integrity analysis was undertaken. This analysis was accomplished to ensure that the resultant designs presented no test hazard to the Transonic Dynamics Facility, the ARES rotor test system, or the associated test personnel. As an integral part of this stress analysis, a failure limit study of the designs was also completed.

No stress levels were predicted or measured during the test which presented a hazard or a limitation to the service life of the model rotor systems.

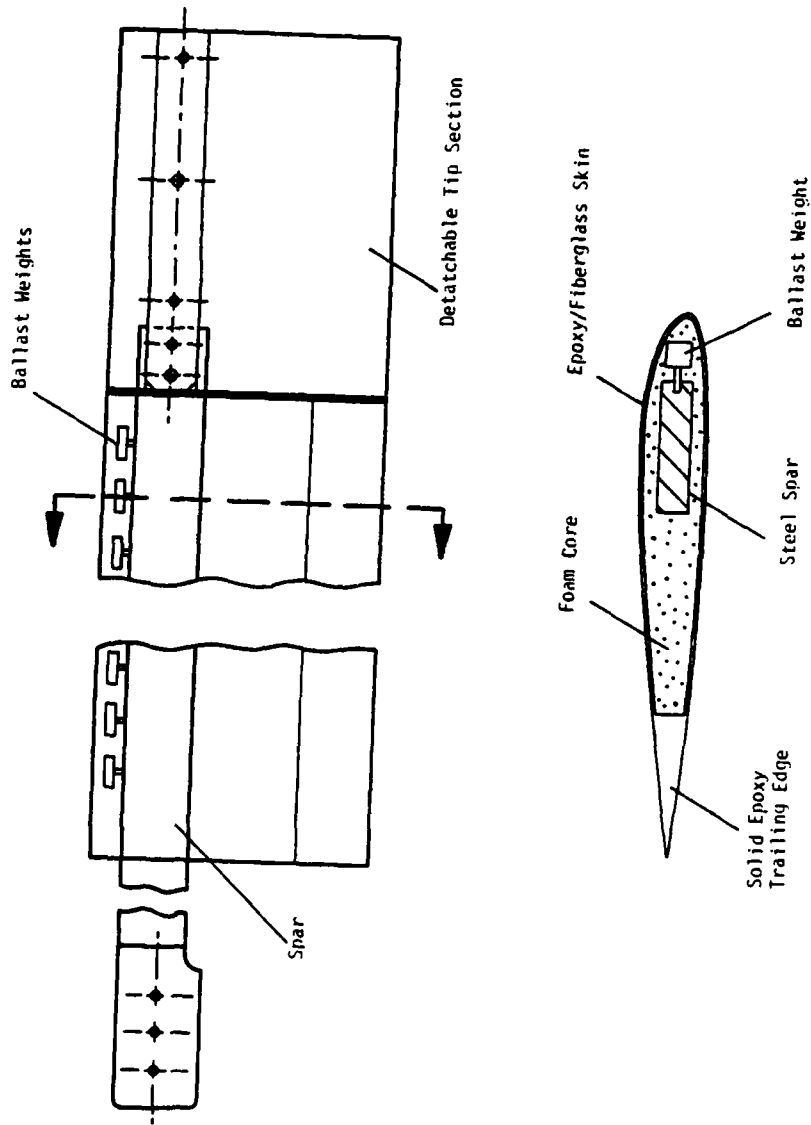


Figure 9. Design Features of Baseline Blade.

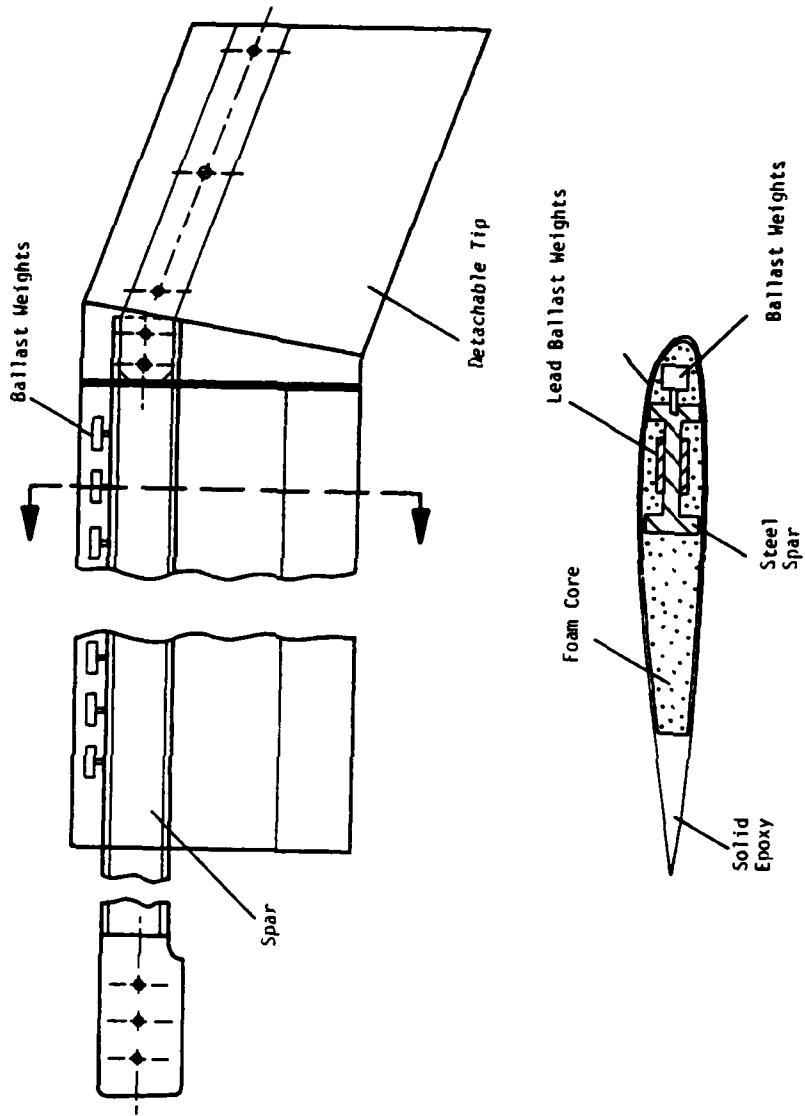


Figure 10. Design Features of ACR Blade.

BLADE FABRICATION

Fabrication Process

The fabrication of the individual baseline and ACR blades generally followed common foam/epoxy/fiberglass composite hand layup practices. The specific fabrication process used is outlined below.

1. Spar Pretwist

The finished machined 17-4 PH (H1150) spar was mounted in a special fixture attached to a granite surface plate and the six-degree tip leading-edge-down twist was achieved by applying a torque (to yield) at the outboard end. All springback was considered so that the six-degree pretwist remained with the spar in a free condition. The pretwist operation was completed prior to drilling the 0.094-inch-diameter ballast weight roll pin holes in the spar forward surface to preclude the occurrence of a nonuniform twist distribution.

2. Spar Drilling

Having completed the pretwist operation, the 0.094-inch-diameter pin holes were drilled in the spar forward surface.

3. Ballast Weights

The individual W2 Kennertium (tungston alloy) weights were drilled for the 0.094-inch-diameter mounting pins. Additional ballast weight was required for the ACR design due to the reduced mass of the H-beam spar. This added weight was attached by bonding lead sheets between the spar flanges.

4. Ballast Weight Installation

The individual ballast weights were mounted to the spar by coating each pin and pin hole with fiber resin No. 7014 structural adhesive and press-fitting the assembly together until the pin bottomed out in both the spar and weight. This procedure established the proper weight offset and positively retained the weights to the spar. Figure 11 shows a typical ballast weight installation and Figure 12 schematically illustrates the static test setup used to confirm the structural integrity of the installation.

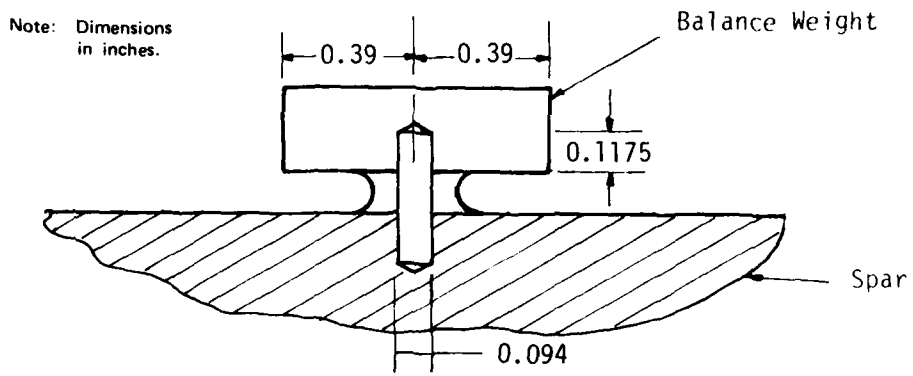


Figure 11. Typical Balance Weight Installation.

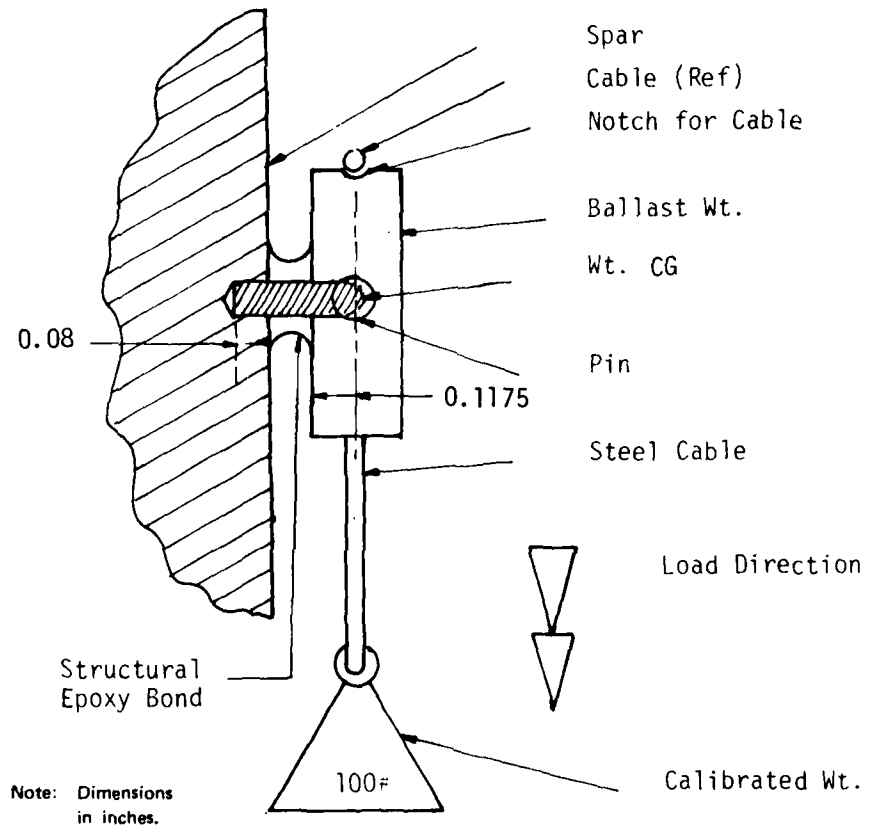


Figure 12. Balance Weight Attachment Test Setup.

5. Blade Instrumentation

One blade of each design was instrumented with flapwise bending, edgewise bending, and torsional strain gauge bridges located at the following positions: 18, 29, 47, and 76 percent forward span.

All gauges were bonded to the spar with Eastman 910 adhesive and encapsulated with Micro-Measurements polyurethane "M" coat "A" to environmentally seal the installation. The specific gauges used were Micro-Measurements No. CEA-06-125UW-350Ω. Each bridge consists of four active legs with the individual elements oriented and interconnected to cancel non-principal axis strains. The blade strain gauge instrumentation was terminated with connectors that mate with the existing NASA/Langley Research Center's ARES model.

6. Airfoil Trailing Edge

To achieve the desired torsional mass moment of inertia, a solid epoxy airfoil trailing edge was designed into the blade composite structure. This trailing edge was manufactured by casting Shell 828/DETA 12 percent epoxy resin in the final blade mold. A special dam was provided to establish the proper chordwise width of the epoxy trailing edge. This cast trailing edge was allowed to cure a minimum of 3 days prior to final blade assembly to insure full strength of the epoxy.

7. Airfoil Foam Core

The foam core of the airfoil consists of two sections. The first is constructed of prefoamed 2-lb/ft³ rigid polyurethane foam. This section fits between the spar aft surface and the forward surface of the epoxy trailing edge piece. The second section of the foam core is foamed in place using 2-lb/ft³ polyurethane Isofoam. This section extends from the blade leading edge to the aft surface of the spar, also filling the open areas between the ballast weights. After attaching the prefoamed section/trailing edge unit to the aft surface of the spar with epoxy resin and free-foaming the forward Isofoam section, the complete airfoil core/spar assembly was rough contoured, using a fixture to establish the basic airfoil shape, twist, and the proper spar location with respect to the 25 percent chord pitch axis. The rough shaped blade was then carefully finished to match the 6-degree linear twisted 23012 airfoil cavity of the blade mold.

8. Final Blade Finish

The final finish construction of the individual rotor blades consisted of applying a 0.004-inch-thick fiberglass cloth/epoxy resin skin to the foam airfoil. This skin was laid up by hand and the complete assembly was placed into the blade mold. The mold established the dimensional properties of the airfoil, the desired linear twist, and the proper location of the spar with respect to the airfoil 25 percent chord pitch axis, and generated the required aerodynamically smooth surface. The complete assembly was allowed to cure a minimum of 36 hours prior to removal from the mold.

9. Tip Construction

Both the rectangular and swept blade tip designs were constructed in a manner similar to the main blade section. In each tip, two aluminum spar plates were bonded to a steel (required for correct mass and CG) chord plate. This spar unit was then covered by a free-foamed polyurethane core and hand finished to a close fit into the proper tip airfoil mold cavity. Once this fitting was completed, the tip unit was skinned with a 0.004-inch-thick fiberglass cloth/polyester resin laminate and allowed to cure in the mold for 12 hours. Two sets of the two tip designs were fabricated. Each individual rotor blade (8 blades total) has a fitted rectangular and swept blade tip. Thus, the tips and blades are not interchangeable. This individual fitting of the tips to each blade ensures the required tight mechanical fit for structural integrity and precludes airfoil discontinuity at the attachment joint.

Molds used in the fabrication process were of a wood/fiberglass construction designed to provide an aerodynamically smooth final surface while maintaining faithful reproduction of dimensional characteristics. These molds were constructed by first building an egg-crate structure from marine plywood with the open portion of the egg crate normal to the mold cavity. The actual mold cavity was constructed by applying an epoxy gel coat over a hardwood master blade pattern (described below). This gel coat provided a smooth defect-free female mold cavity. On top of the gel coat, several layers (approximately 0.25 inch thick) of fiberglass tooling cloth were laid up with epoxy resin. The last step in the mold construction was completed by bonding the egg-crate reinforcing structure to the fiberglass mold cavity. Two such rotor blade molds, the rectangular tip mold and the swept tip mold, were constructed in this manner.

A separate mold of 24-inch length, without blade twist, was constructed of hardwood for the fabrication of the test and evaluation blade sections.

The construction of the master pattern was based on a series of metal airfoil templates. These templates, after fabrication, were inspected using a three-dimensional measurement machine to ensure faithful reproduction of the 23012 airfoil ordinates. The resulting inspection report indicated that all of the templates were within a maximum variation of 0.002 inch of specified ordinates. Using these templates and a fabrication jig that established the 6-degree linear blade twist distribution, a male hardwood master blade pattern was constructed. This pattern was laminated so that warpage was precluded. The master pattern was used to layup all final mold cavities.

Model Blade Characteristics

The baseline and ACR model rotor blades in their final form were extensively inspected and tested to ensure that each individual unit met both the required mechanical properties and physical characteristics. These tests included static and dynamic (natural frequency) investigations as well as a carefully completed weight balance procedure to preclude operational vibration and tracking problems during the wind-tunnel test. A calibration of the strain gauges installed on one blade of each design was also completed. The following section outlines the testing undertaken to establish the final blade characteristics.

The procedure established was based on a fifth complete blade of each design, used for final confirmation of the systems. These were the first complete blades to be fabricated. Construction of the actual four-blade wind-tunnel sets were not started until after acceptance of the test blades.

7
B

The specific testing of the acceptance blades included a series of calibrated static dead weight loadings to establish the flapwise, edgewise, and torsional stiffness characteristics. These tests were conducted in the same manner as the sample section tests undertaken during the iterative design phase. Figure 13 shows a typical setup using the specially designed fixtures.

Further confirmation of the mechanical properties of the designs through the use of the completed final test blade was obtained by checking the natural frequency response. This test setup is shown in Figure 14, which depicts the 2-pound shaker attached to the blade root fitting (simulated pitch housing).

The test blade response was measured using a small (very low mass) accelerometer attached with double-sided tape. The output of the accelerometer/charge amplifier system was displayed on a multichannel oscilloscope along with the shaker input signal for monitoring resonance points. Prior to these tests, the HASTA analysis (Reference 69.) was used to predict the frequency response of the designs. Table 8 provides a comparison of the test results for the baseline blade with the prediction. Because of the

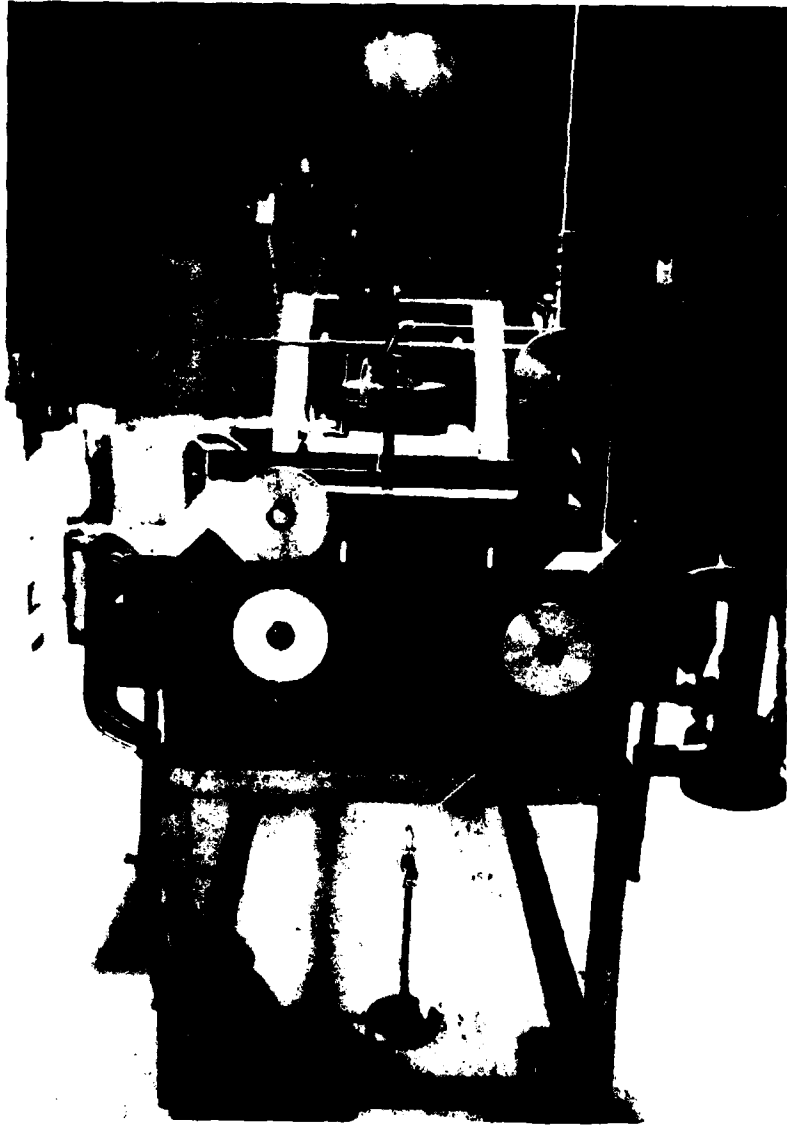


Figure 13. Static Deflection (Spar) Test Setup.

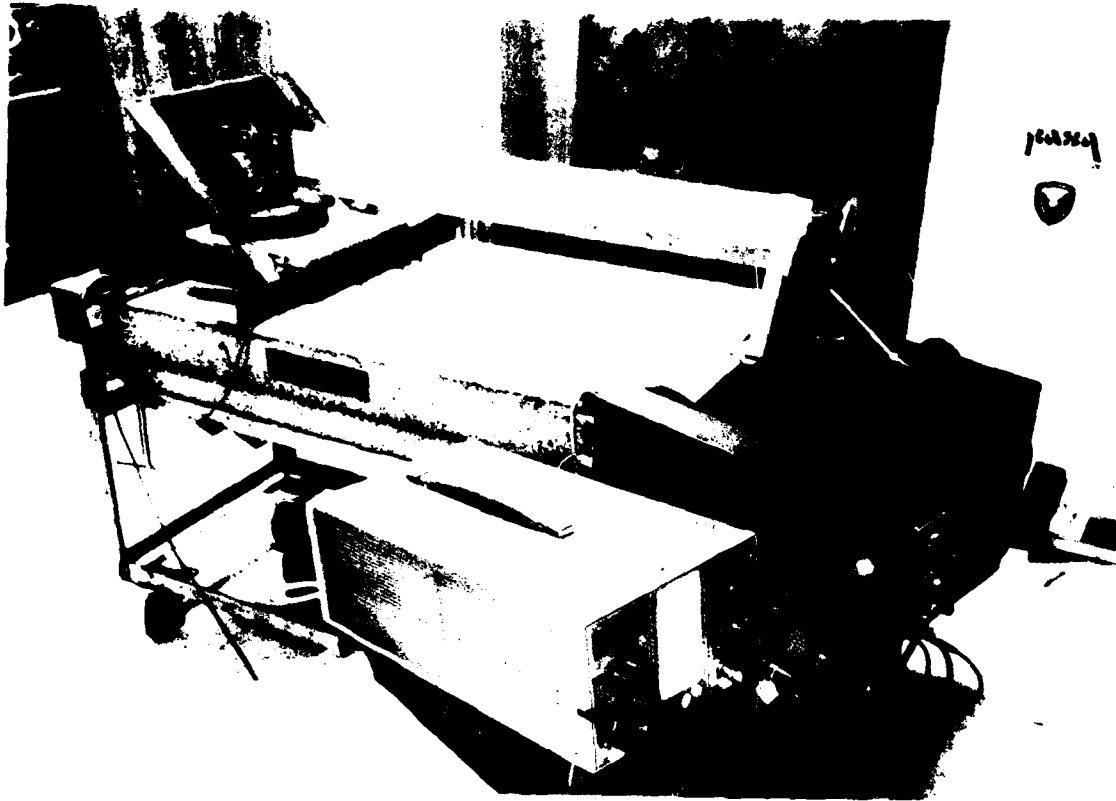


Figure 14. Vibration Test Setup.

good correlation obtained between the measured and predicted frequencies of the baseline blade, only a brief investigation to obtain the measured frequencies of the ACR blades was made. On the basis of this investigation, which only roughly determined the fundamental frequencies in flapwise and edgewise bending, it was concluded that the predicted frequencies for the blades could be used to represent the vibratory characteristics of these blades. In conjunction with the vibration tests, a careful study was made of the node points of the various modes. These node points were determined by selected placement of the accelerometer and visual examination using a strobe light set slightly off frequency. The strobe light, set a few Hertz off the modal frequency, allowed the relative moment of the vibrating blades to be viewed in slow motion. All node points were found to be at or near the predicted positions.

TABLE 8. BASELINE BLADE NONROTATING FREQUENCIES, HZ

<u>Mode Type</u>	<u>Measured</u>	<u>Predicted</u>
1st Flapwise	4.10	4.14
2nd Flapwise	26.30	25.90
3rd Flapwise	73.50	72.70
4th Flapwise	140.00	142.70
1st Chordwise	14.50	16.70
2nd Chordwise	110.00	104.60
3rd Chordwise	320.00	292.80
1st Torsion	103.00	95.00
2nd Torsion	275.00	285.00
3rd Torsion	455.00	474.90

During the acceptance tests, a great deal of effort was expended to measure accurately the shear center of the test blades. This undertaking, although not totally successful because of the problems associated with the inter-axis coupling of the 8-degree built-in blade twist, did confirm the actual shear center to be at or near the required 25 percent chord position. Further confirmation of this axis location was made during the strain gauge calibration tests.

After the final blade design testing was successfully completed, the two sets of actual wind-tunnel test blades, along with their interchangeable tips, were fabricated. All blades and tips were checked out in a similar manner to assure that no differences existed blade-to-blade within a given set (e.g., all baseline blades exhibited the same characteristics).

Balancing of the blade sets was accomplished using a three-step procedure. The first step matched the total weight of all blades in a test set. The interchangeable blade tips were also weight-balanced in the same manner. The final test blades were all within a narrow total variance and required only minor corrections because of the careful weight matching of all individual components during the fabrication process.

The second and third operations established the spanwise CG locations for each blade set. These operations were accomplished by fitting one end of the blade with a knife edge perpendicular to the pitch axis and installing a single point support at the opposite end of the blade. The single point was then placed in the center of the pan of a precision balance and minor ballasting added to achieve the same cantilevered weight for each blade in the set. This procedure was completed for both ends of each blade. The final balancing was completed with the interchangeable tips installed so that no CG shift occurred because of configuration changes.

The accuracy of this balance procedure was illustrated by the absence of any balance problems or excessive vibration during both the hover stand and wind-tunnel testing of the two rotor systems.

During the final acceptance tests of the actual test articles, the instrumented blades from both the baseline and ACR sets were calibrated. This calibration was accomplished using dead weight static loadings and recording the inch-pound per millivolt per volt output of the strain gauge bridges at each of the three spanwise locations. These data were supplied with the test blades at the time of the installation on the ARES test system.

WIND-TUNNEL TESTS

Test Purpose and Procedures

The purpose of the test program was to evaluate the benefits of the ACR design concept over a range of advance ratios and thrust loadings. This evaluation was accomplished by testing both the conventional blade set (baseline) and the blade set that was designed using the ACR concept at comparable rotor force and moment condition. Comparison of the test results obtained with each set then permitted the evaluation of the benefits achieved by using the ACR concept. Prior to the wind-tunnel tests, a brief program was conducted on a hover test stand to check the operation of the system and blade track. Both the hover and wind-tunnel tests were conducted by NASA using the ARES helicopter model in the Transonic Dynamics Test Facility at NASA/Langley. Figure 15 shows the four-bladed swept-tip configuration mounted in the wind tunnel. The tape on the leading and trailing edges was not present during the test. Table 9 presents the configurations that were available for test and the ones that were tested during the wind-tunnel tests in a Freon environment.

TABLE 9. TEST CONFIGURATIONS

<u>Test Configuration</u>	<u>Rectangular Tip</u>	<u>Swept Tip</u>
Four-Bladed Baseline	Tested	Not tested
Four-bladed ACR	Tested	Tested
Two-Bladed Baseline	Tested	Not Tested
Two-Bladed ACR	Not Tested	

As can be seen from Table 9, just over half of the configurations available for test were actually tested, based on order, priority, and test time available.

The data that were recorded and documented during the test programs are as follows:

Wind-tunnel test conditions: M_N , q , velocity, temperature, Freon purity

Six components of steady balance data: N_F , D_F , F_S , M_p , M_R , M_Y

Blade flapping motion: Steady and eight harmonics

Blade lead-lag motion: Steady and eight harmonics

Pitch link load: Steady and eight harmonics

Blade collective pitch: Steady and eight harmonics

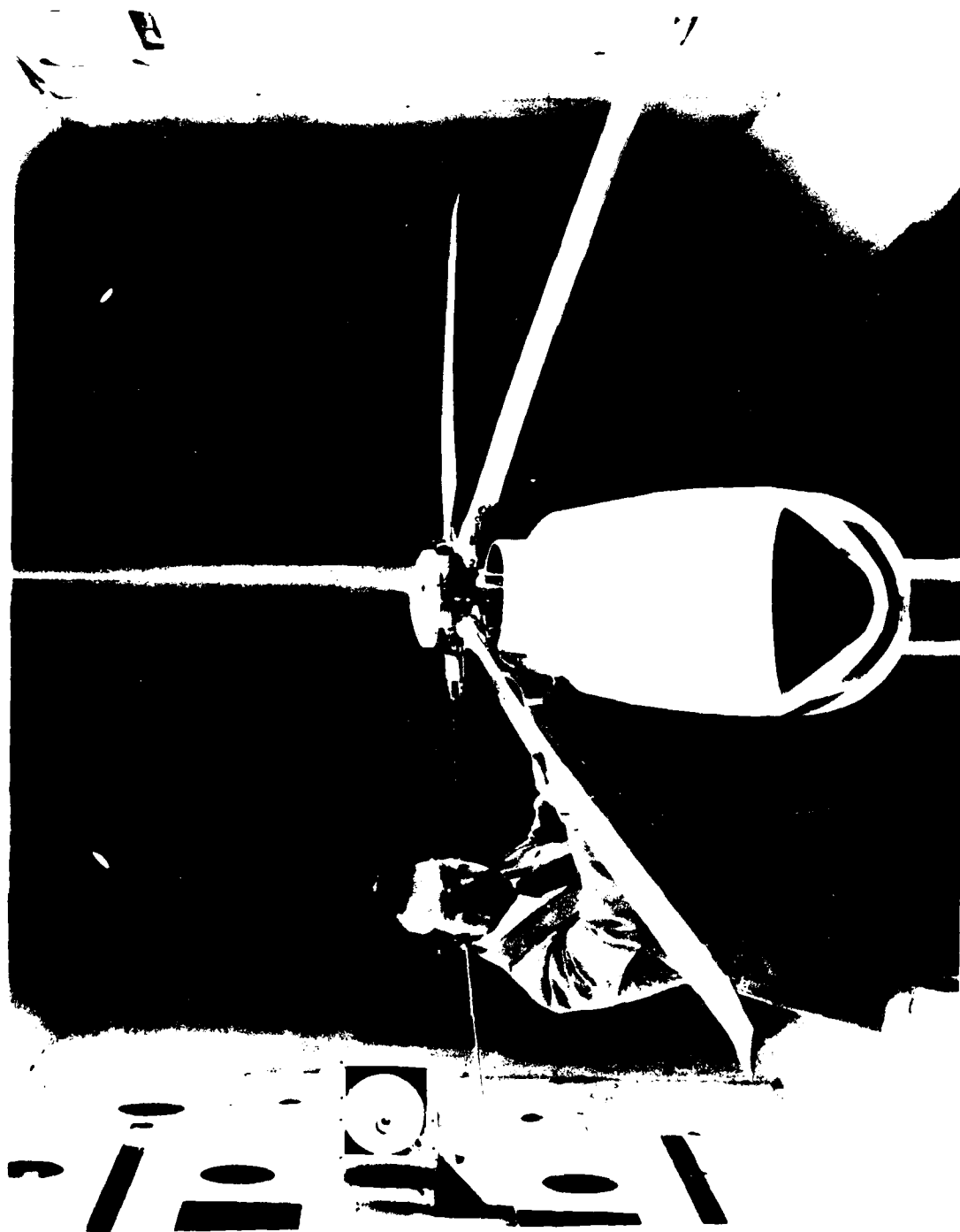


Figure 15. ACR Swept-Tip Blades Mounted in the NASA Transonic Dynamics Tunnel.

Blade longitudinal cyclic pitch: Steady and eight harmonics
Blade lateral cyclic pitch: Steady and eight harmonics
Blade flapwise bending moment at 18, 29, 47, and 76 percent R:
Steady and eight harmonics
Blade edgewise bending moment at 18, 29, 47, and 76 percent R:
Steady and eight harmonics
Blade torsional moment at 18, 29, 47, and 76 percent R:
Steady and eight harmonics
Shaft angle to airstream

The tests were conducted by flying the model to a prespecified aircraft trim condition that had been calculated by the C81 computer program. While these trim conditions are limited by the theory, they did provide a set of conditions that represented loadings that a rotor system must develop in flight to trim a helicopter in steady-state operation. In general, for a given test configuration, the thrust was increased in steps at a given advance ratio. At each thrust value, a trim condition was established prior to gathering the test data. These experimental trim points were obtained by manual iteration to the desired combination of forces which is considerably more time consuming than the traditional procedure of performing collective pitch and shaft angle sweeps with no flapping. This procedure substantially limited the number of configurations, thrust levels, and advance ratios that could be tested, but was selected because each data point is independent, meaningful, and interpolation of final results is not required. The prespecified trim conditions were found to be obtainable with the model up to levels of thrust where blade loads or power required were considered to be excessive.

Discussion of Experimental Results

Figure 16 presents the basic results obtained for the various configurations at an advance ratio of $\mu = 0.25$, while Figure 17 presents similar results at $\mu = 0.35$. In comparing the results for the four-bladed configurations for $\mu = 0.25$, it can be seen that for C_T/σ 's less than 0.10, the baseline blade had performance characteristics superior to either of the ACR configurations. Above $C_T/\sigma = 0.10$, however, the performance characteristics of the baseline rotor configuration deteriorate rapidly and both ACR blade configurations become increasingly superior as the thrust increases. At a C_T/σ of 0.1125, for example, the ACR swept-tip configuration develops the same thrust as the baseline blade while using only about 70 percent of the horsepower. While the ACR blades with the rectangular tip have better performance characteristics than the baseline blades above a C_T/σ of 0.10, they are inferior to the ACR configuration with swept tips. In comparing the apparent stall-induced power losses for the three four-bladed configurations, it can be seen that they start to occur at a C_T/σ of approximately

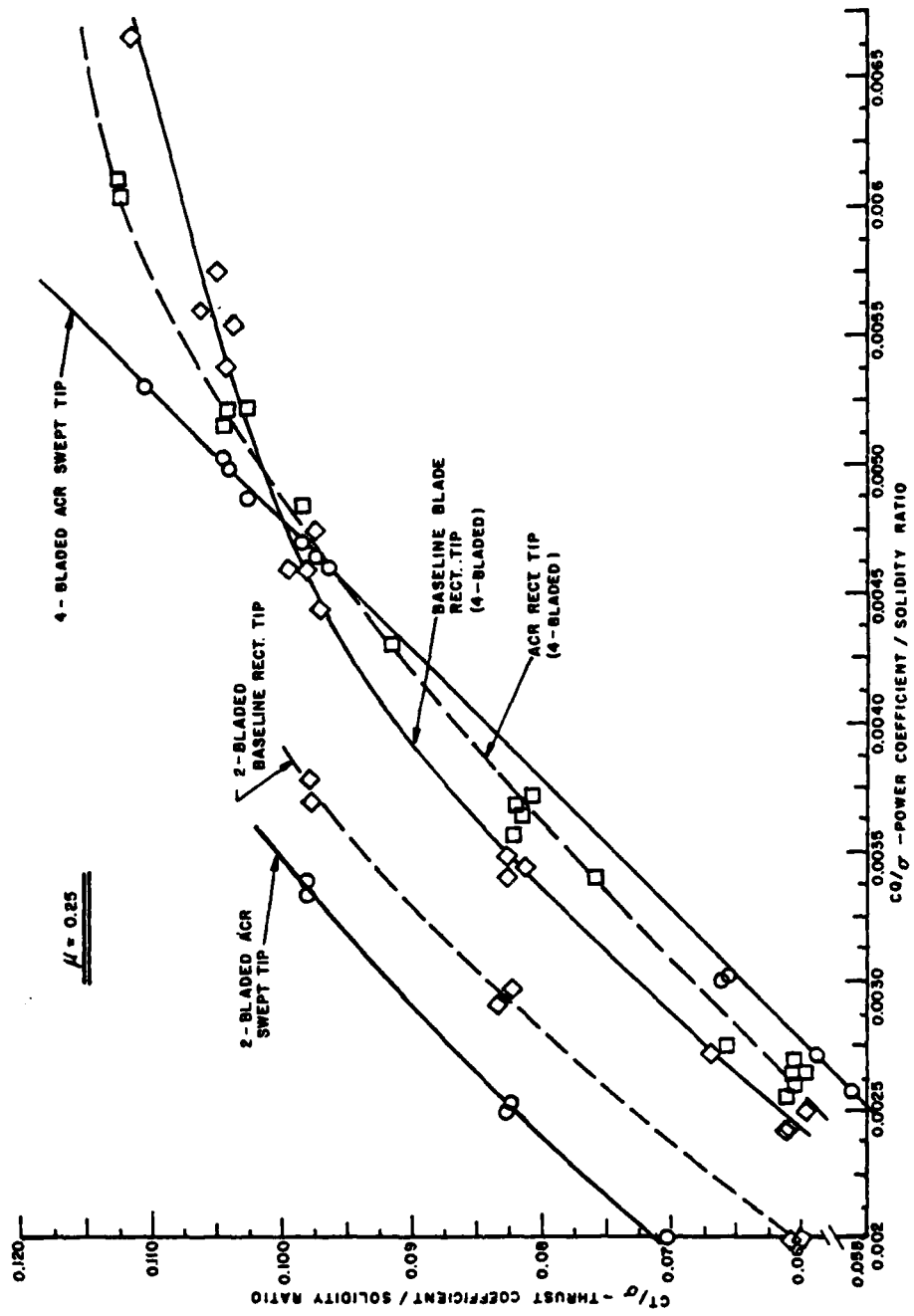


Figure 16. Coefficient of Thrust/Solidity Ratio vs. Coefficient of Power/Solidity Ratio - $\mu = 0.25$.

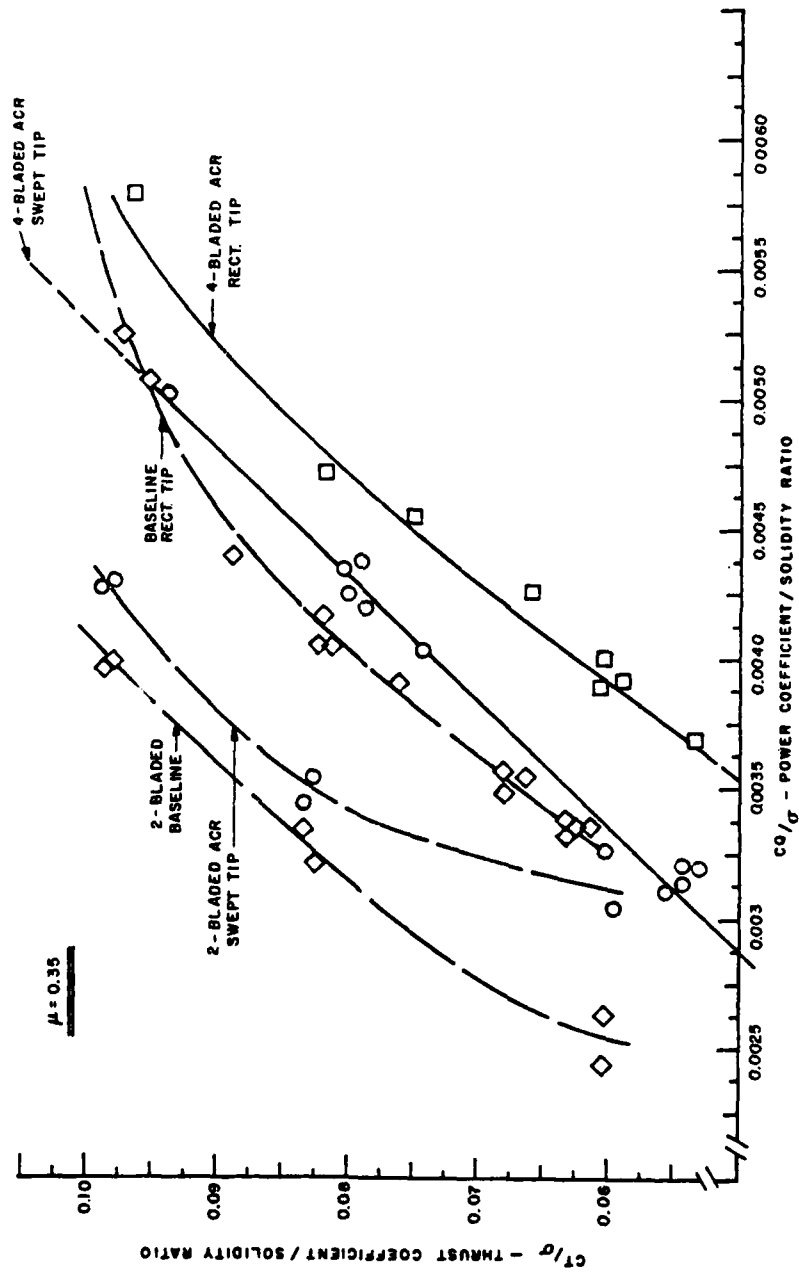


Figure 17. Thrust Coefficient/Solidity Ratio vs. Power Coefficient/Solidity Ratio - $\mu = 0.35$.

0.090 for the baseline blade, at 0.095 for the ACR rectangular tip configuration, and are not noticeable for the ACR configuration with swept tips. The ACR blades with swept tips were not tested to high enough values of C_T/σ so that the point at which the power loss due to stall becomes noticeable could be determined. It is apparent from the data obtained, however, that the C_T/σ at which this would occur with the ACR swept-tip configuration is much higher than that obtained for either the baseline blades or the rectangular-tip ACR blades. The performance crossover point would probably occur at lower values of C_T/σ for ACR blades with the originally desired torsional stiffness.

The results obtained for both of the two-bladed configurations at a $\mu = 0.25$ (Figure 16) indicate that their nondimensional performance characteristics are superior to any of the four-bladed configurations. For example, at a C_T/σ of 0.095 the two-bladed baseline blade with rectangular tips uses 16.5 percent less nondimensionalized power than the four-bladed baseline configuration and the two-bladed ACR design with swept tips uses only 60 percent of the nondimensionalized power required by its four-bladed counterpart. This significant increase in performance is believed to be due to the more favorable wake environment of the two-bladed rotor configurations due to blade/vortex spacing and the reduced rotor thrust. It is also apparent that at $\mu = 0.25$, the ACR blade interacts with the wake in a more favorable manner than the baseline blade since the two-bladed ACR configuration shows more than twice the benefit of the baseline design over their four-bladed counterparts. Based on the limited data that were obtained with the two-bladed configurations, both the baseline and ACR blades seem to indicate the effects of stall at the highest value of C_T/σ that was obtained. This characteristic is different than that obtained with the four-bladed ACR configuration having a swept tip. A complete assessment of the effect of number of blades with regard to ACR would require testing of a two-bladed configuration with twice the chord and testing well into stall to establish performance limits.

At an advanced ratio of $\mu = 0.35$, the performance characteristics of the various rotor configurations show similar trends to those obtained at $\mu = 0.25$, but with some significant differences. The four-bladed ACR swept-tip rotor again has poorer performance characteristics at C_T/σ 's less than 0.095, but the trends indicated by the data show that the ACR design will have significantly improved performance characteristics over those of the baseline blade above a C_T/σ of 0.095. At $\mu = 0.35$, test data were not obtained at as high a C_T/σ as $\mu = 0.25$, so definitive trends of the rotor performance at the higher thrust coefficients could not be evaluated. A major difference in the performance characteristics of the four-bladed ACR with the rectangular tips was obtained at $\mu = 0.35$, in that its performance characteristics were inferior to those of the ACR swept tip over the entire range of C_T/σ 's for which data were obtained. Inspection of the data did not reveal any obvious reasons for this significant change in the performance characteristics between $\mu = 0.25$ and $\mu = 0.35$.

While the two-bladed configuration had superior performance over their four-bladed counterparts at $\mu = 0.35$, it is noted that the baseline blade had better performance characteristics than the swept-tip ACR design; this is just the opposite of their relationship at $\mu = 0.25$. Again, the reason for this significant difference could not be found by analysis of the data.

A major conclusion that can be reached from the data presented in Figures 16 and 17 is that the benefits achieved by the ACR design with the swept tip at the higher coefficients of thrust were those predicted by the theoretical design analyses conducted early in the research program. While significant benefits were obtained with the ACR rotor configuration, greater benefits might have been demonstrated if the rotors had been constructed to achieve the full stiffness reductions upon which the theoretical blade designs were based.

Figure 18 presents the performance data in a slightly different format, which more clearly portrays the rotor efficiency as a function of the rotor thrust. At $\mu = 0.25$, C_T/C_Q is about constant over the range of C_T for which data were obtained for the ACR design with swept tips, while C_T/C_Q continually decreases as C_T increases for the ACR design with the rectangular tip and for the baseline rotor. At $\mu = 0.35$, C_T/C_Q increases with C_T for both of the ACR designs, while only the baseline rotor system shows a decreasing efficiency at the higher values of C_T . While the maximum value of C_T/C_Q is less at $\mu = 0.35$ than it is at $\mu = 0.25$, the maximum values of C_T/C_Q are significantly greater at both advance ratios when compared with those reported in References 15 and 16 for other ACR blade designs. When comparing the data at $\mu = 0.35$ with that of $\mu = 0.25$, it is apparent that the ACR designs might also be significantly better than the baseline blades at the higher thrust coefficients at $\mu = 0.35$. That these benefits occur only at high blade loadings is directly attributable to the ACR blades higher than desired torsional stiffness.

The oscillatory flapwise bending moments at 18 percent of radius as a function of the thrust for the various blade configurations are presented in Figures 19 and 20 for $\mu = 0.25$ and $\mu = 0.35$, respectively. In comparing the results at $\mu = 0.25$ and $\mu = 0.35$, it can be seen the general trends of the oscillatory bending moments as well as their magnitudes are significantly different at the two advance ratios. At $\mu = 0.25$, the oscillatory bending moment continually increases with increasing thrust, but at $\mu = 0.35$, the moments seem to reach a maximum value at an intermediate value of thrust and then start to decrease as the thrust is increased further. Since the differences in trends are apparent for all configurations for the two advance ratios, they must be attributable to the difference in the aerodynamic environment in which the blades are operating rather than the blade design. Additional data at closer intervals and at higher thrusts are needed to firmly establish the trends of the flapwise bending moment with thrust at $\mu = 0.35$. It is also noted that the magnitude of the oscillatory bending moments are significantly higher at $\mu = 0.35$. While this is

15. Blackwell, R. H., INVESTIGATION OF THE COMPLIANT ROTOR CONCEPT, Sikorsky Aircraft; USAAMRDL TR 77-7, Eustis Directorate, USAAMRDL, Fort Eustis, Virginia, June 1977, AD A042338.

16. THE DEVELOPMENT AND APPLICATION OF AN ANALYSIS FOR THE DETERMINATION OF COUPLED TAIL ROTOR/HELICOPTER AIR RESONANCE BEHAVIOR, RASA Division, Systems Research Laboratories, Inc.; USAAMRDL TR 75-35, Eustis Directorate, USAAMRDL, Fort Eustis, Virginia, August 1975, AD A014989.

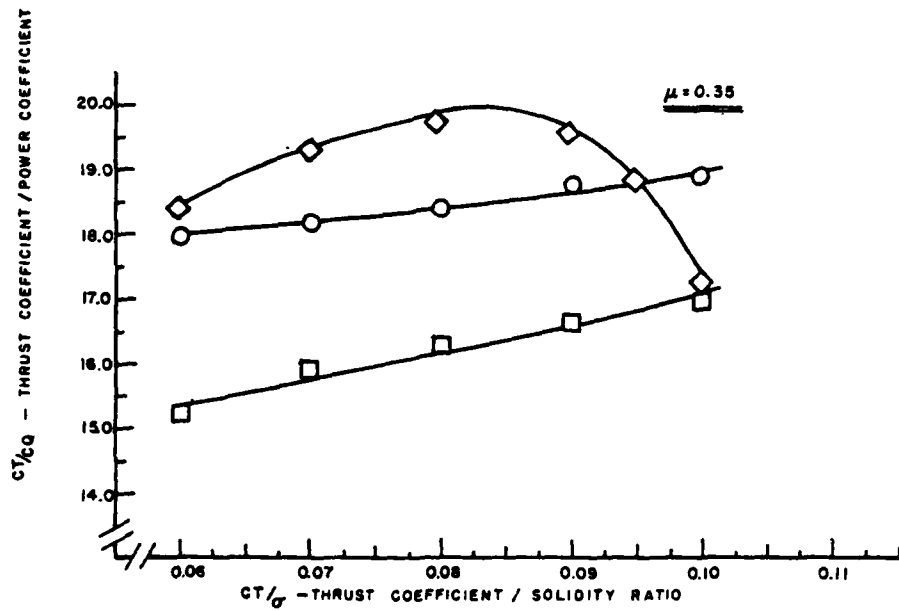
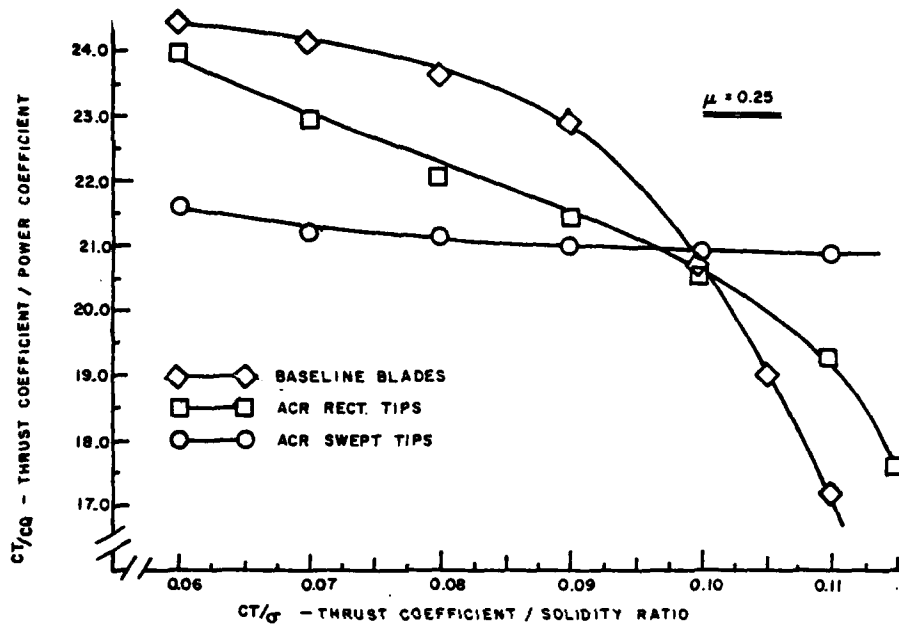


Figure 18. CT/CQ vs. CT/σ for Four-Bladed Rotors.

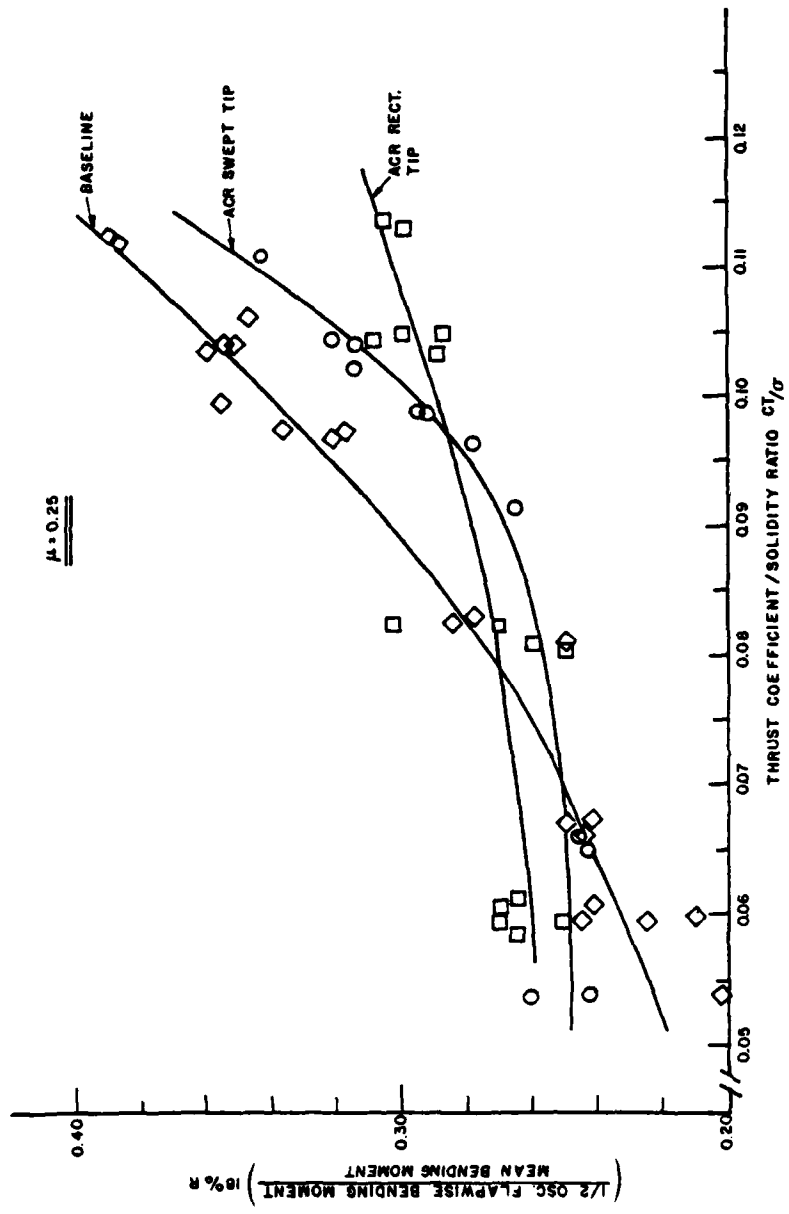


Figure 19. Nondimensional Oscillatory Flapwise Bending Moment at 18% Radius vs. Thrust Coefficient/Solidity Ratio for $\mu = 0.25$.

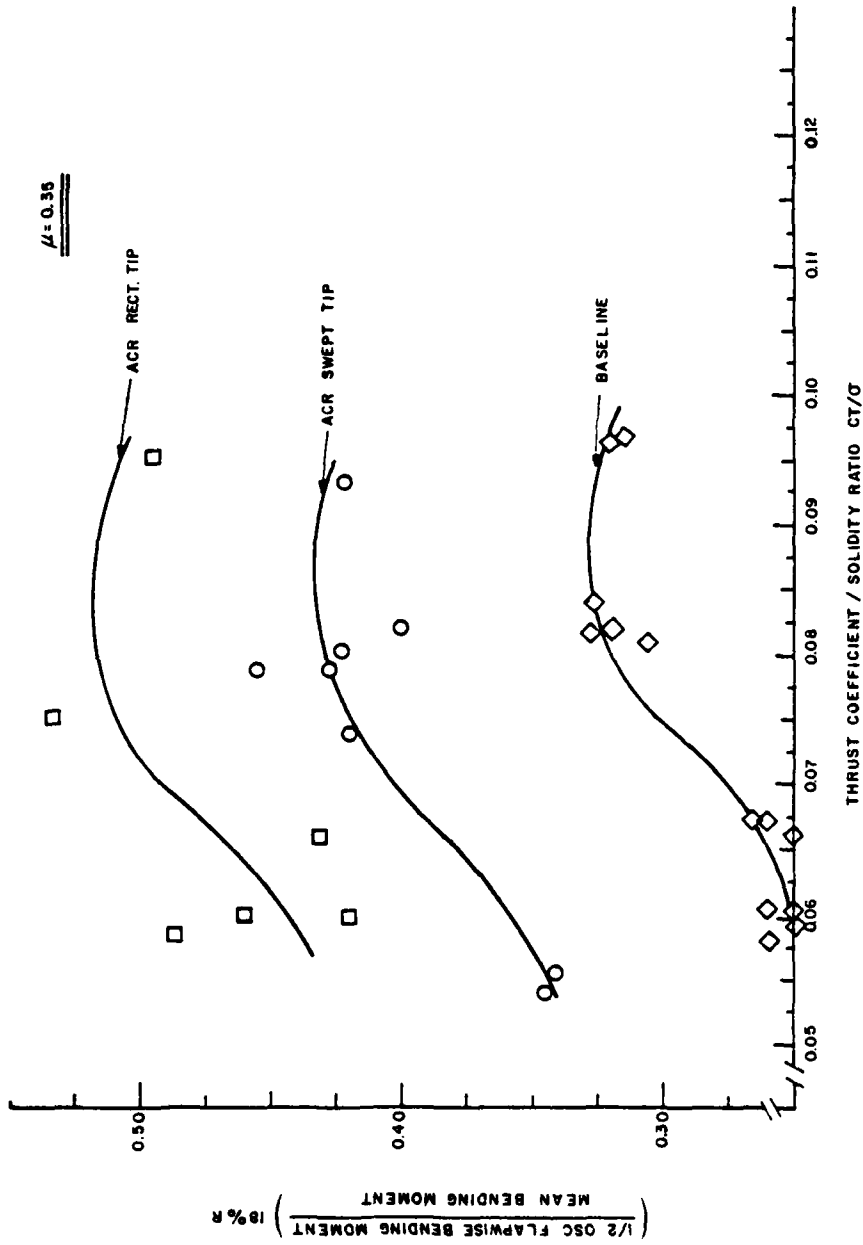


Figure 20. Nondimensional Oscillatory Flapwise Bending Moment at 18% Radius vs. Thrust Coefficient/Solidity Ratio for $\mu = 0.35$.

to be expected, the relative magnitudes of the oscillatory bending moments for the various blade configurations at $\mu = 0.35$ are significantly different from those which were noted at $\mu = 0.25$. At the highest value of C_T/σ obtained at $\mu = 0.35$, the bending moment of the ACR swept tip configuration is only 80 percent of that of the rectangular ACR tip configuration, while at $\mu = 0.25$ they had approximately the same value. At that same value of C_T/σ , the oscillatory moment of the baseline blade was 20 percent higher at $\mu = 0.25$, but 40 percent lower than the ACR rectangular tip design at $\mu = 0.35$. The reason for this significant shift in the relative magnitudes of the oscillatory bending moments could not be determined from the analysis of the data.

Similar results and comparisons are noted for the oscillatory edgewise moments measured for the various configurations at $\mu = 0.25$ and 0.35 ; these data are presented in Figures 21 and 22 respectively. It is noted from a comparison of the data in Figures 21 and 22 that the trends of the oscillatory edgewise bending moment are the same at $\mu = 0.25$ and $\mu = 0.35$; i.e., oscillatory bending moment increases with increasing C_T/σ . It is also noted that while the oscillatory bending moments at $\mu = 0.25$ are approximately the same, at $\mu = 0.35$ the oscillatory bending moment of the ACR swept-tip configuration and the ACR rectangular tip configurations are approximately 40 percent and 90 percent higher, respectively, than the baseline configuration.

The oscillatory torsional moments for the three different configurations at advance ratios $\mu = 0.25$ and $\mu = 0.35$ are presented in Figures 23 and 24 respectively. At $\mu = 0.25$, the oscillatory torsional moment is approximately the same for all blade configurations and increases with increasing thrust. However, since the torsional stiffness of the ACR blades is approximately one-fourth of that of the baseline blades, the oscillatory deflections of the ACR blades are on the order of four times that of the baseline blade.

At $\mu = 0.35$, the oscillatory torsional moments of the baseline and ACR blades with the rectangular tips increase with thrust, while those of the ACR swept-tip design tend to remain constant or to decrease slightly. An attempt was made to correlate the difference in behavior of the oscillatory torsional moments (deflections) between $\mu = 0.25$ and $\mu = 0.35$, with the differences noted in the flapwise and edgewise oscillatory moments, but no definitive correlation could be established.

The oscillatory bending and torsional moment data obtained for the two-bladed baseline and ACR swept-tip rotor designs at $\mu = 0.25$ and $\mu = 0.35$ are shown in Figures 25 through 27. In comparing the two-bladed data with the four-bladed data, it can be seen that the oscillatory magnitudes of the moments and the trends with thrust and advance ratio are approximately the same. This observation indicates that, while the data was limited in this test series, the noted trends of experimental data are probably correct.

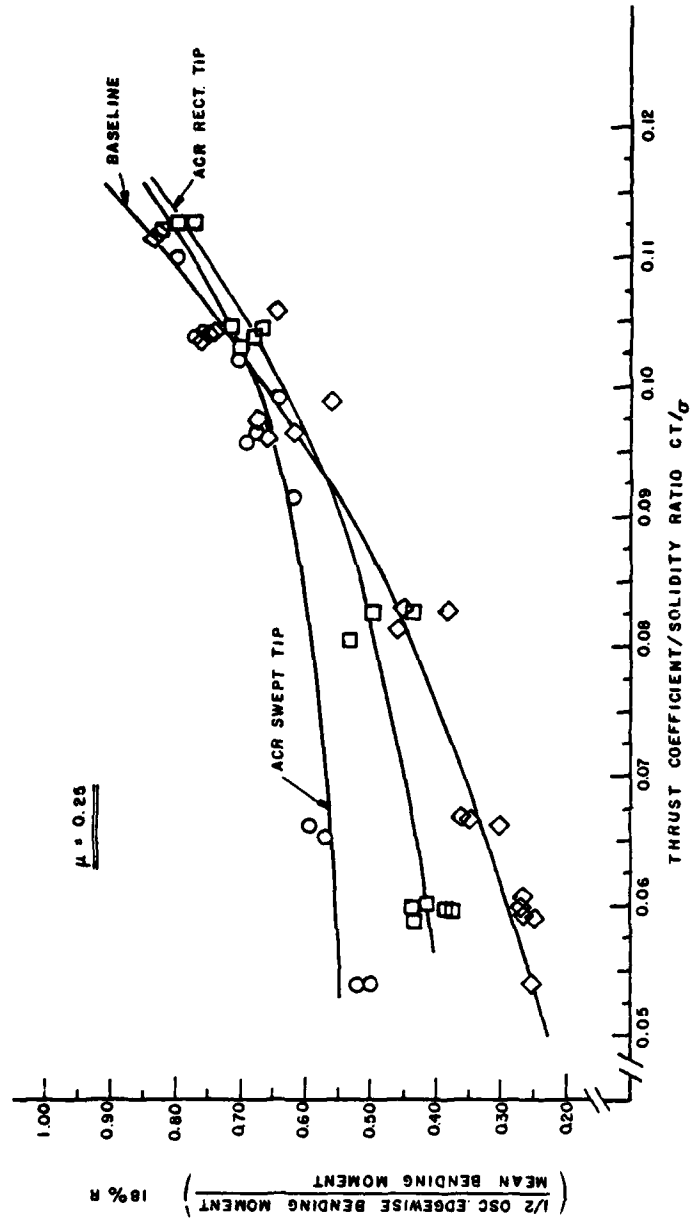


Figure 21. Nondimensional Oscillatory Edgewise Bending Moment at 18% Radius vs. Thrust Coefficient/Solidity Ratio for $\mu = 0.35$.

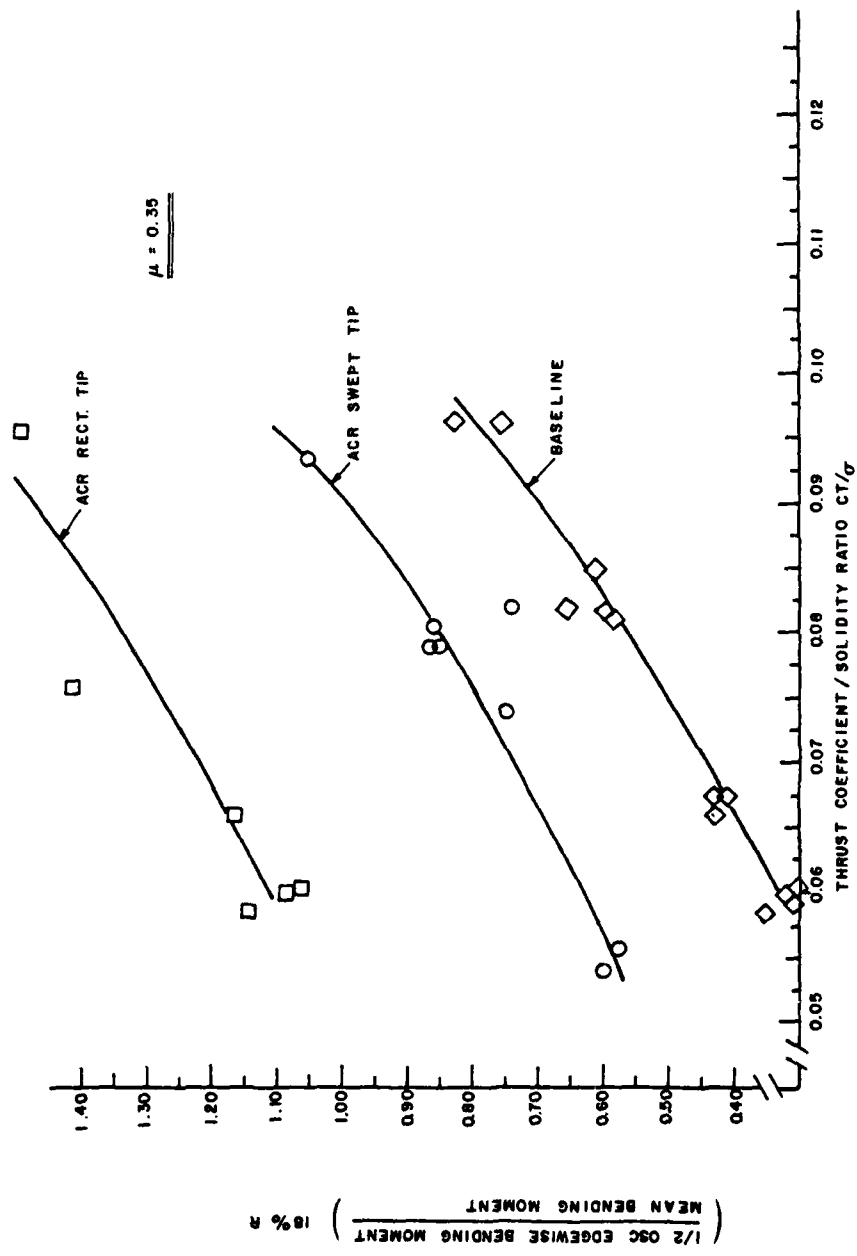


Figure 22. Nondimensional Oscillatory Edgewise Bending Moment at 18% Radius vs. Thrust Coefficient/Solidity Ratio for $\mu = 0.35$.

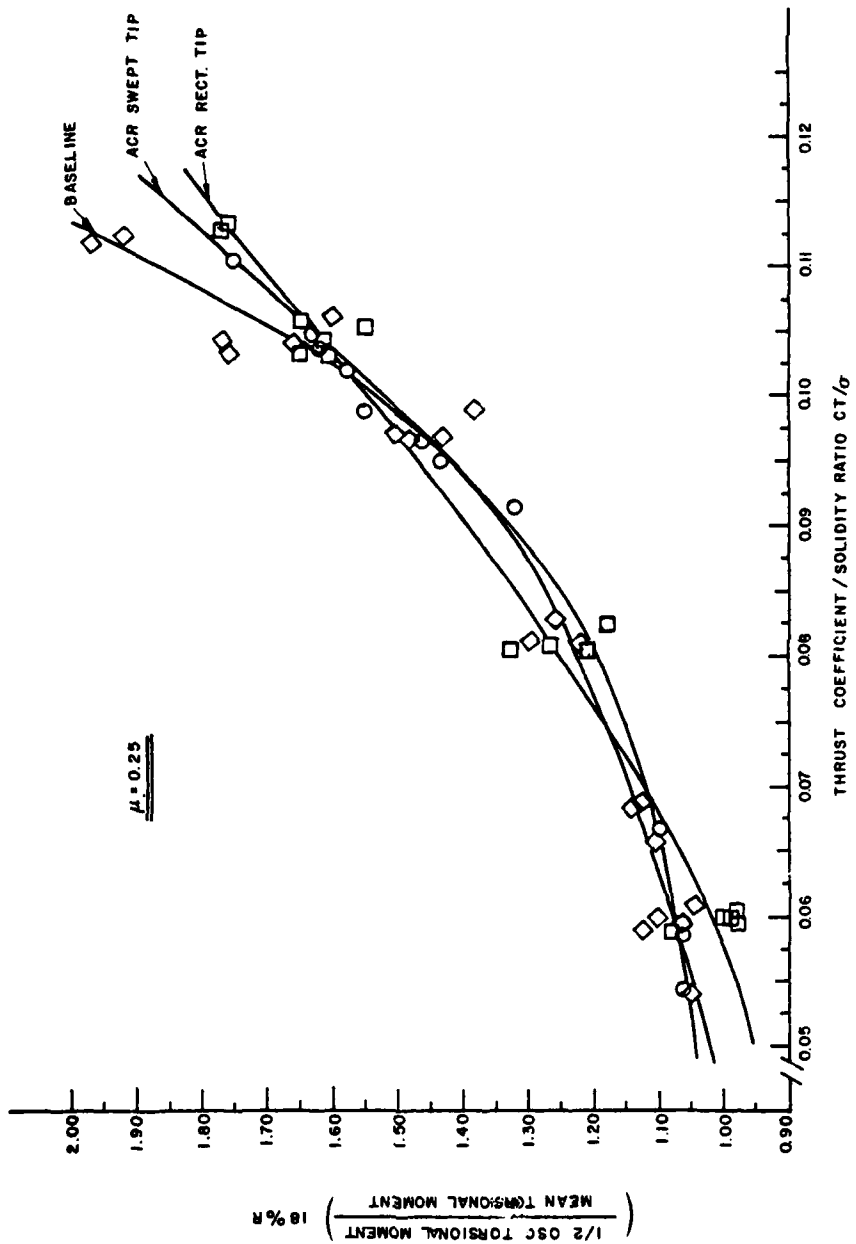


Figure 23. Nondimensional Oscillatory Torsional Moment at 18 Radius vs. Thrust Coefficient/Solidity Ratio for $\mu = 0.25$.

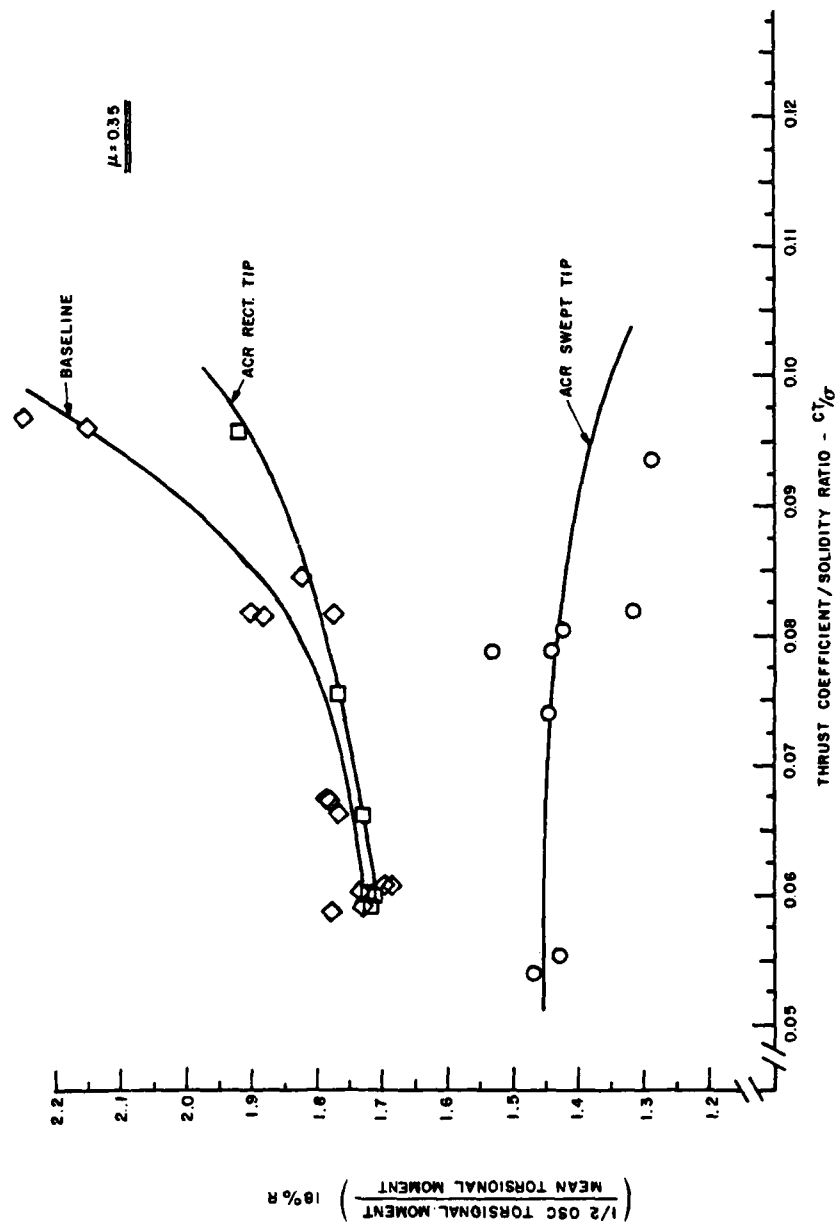


Figure 24. Nondimensional Oscillatory Torsional Moment at 18% Radius vs. Thrust Coefficient/Solidity Ratio for $\mu = 0.35$.

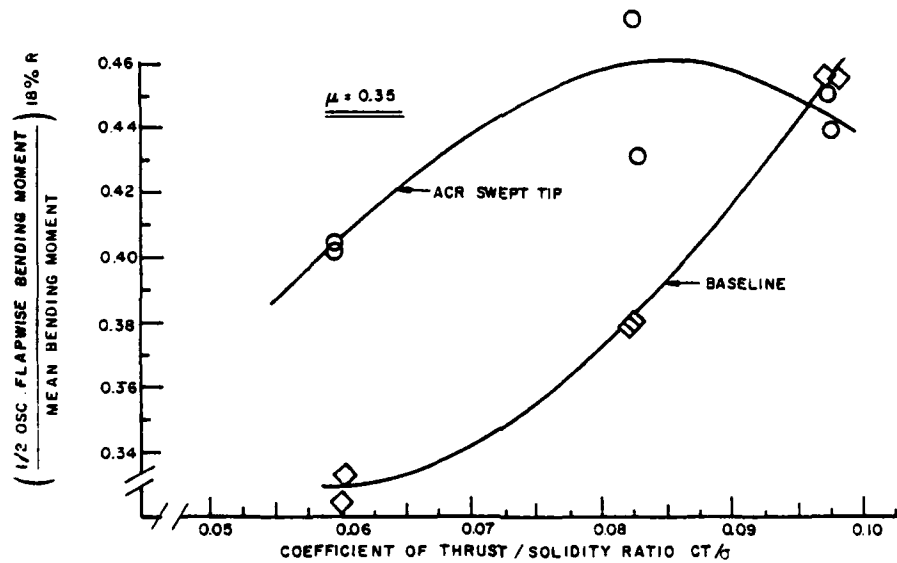
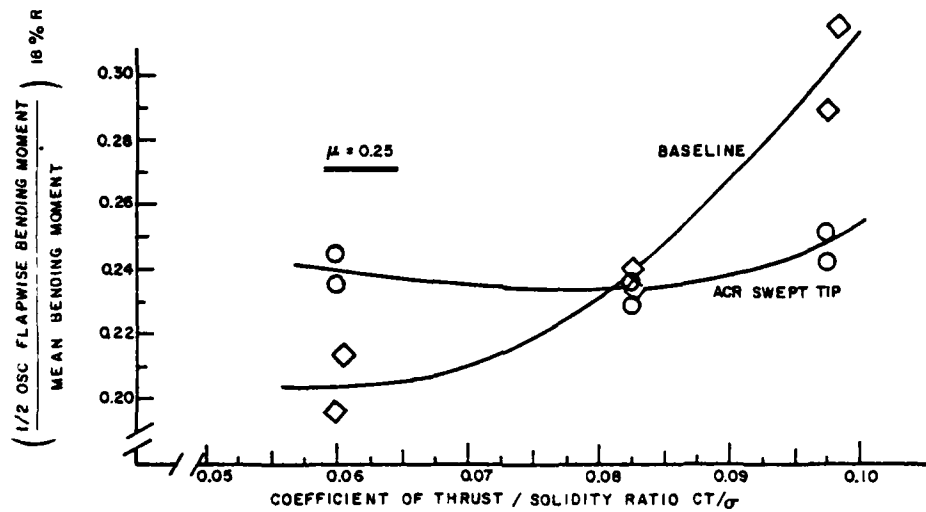


Figure 25. Oscillatory Flapwise Bending Moment vs. CT/σ for Two-Bladed Rotors.

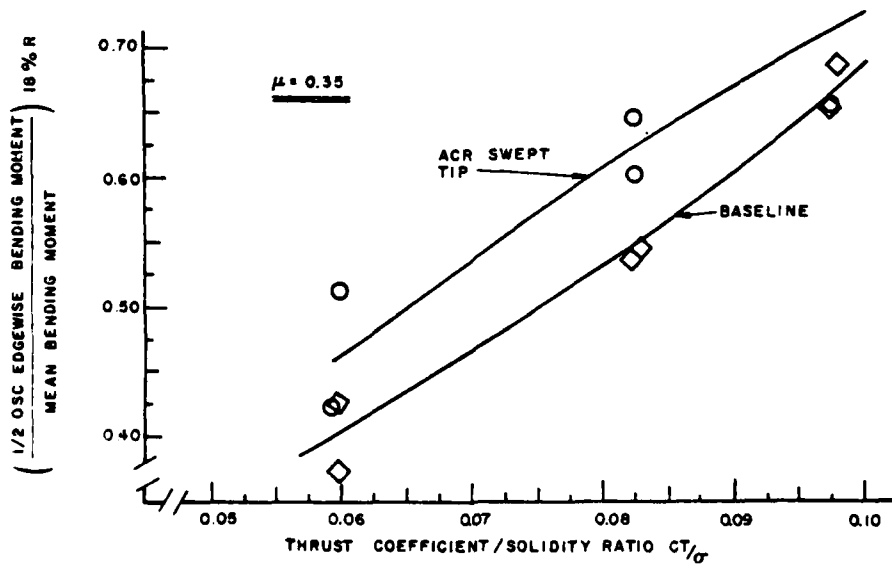
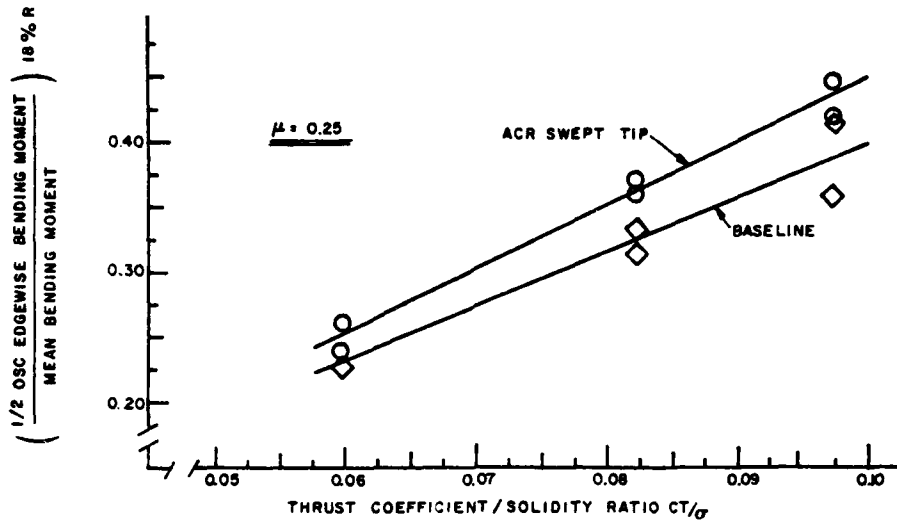


Figure 26. Oscillatory Edgewise Bending Moment vs. CT/σ for Two-Bladed Rotors.

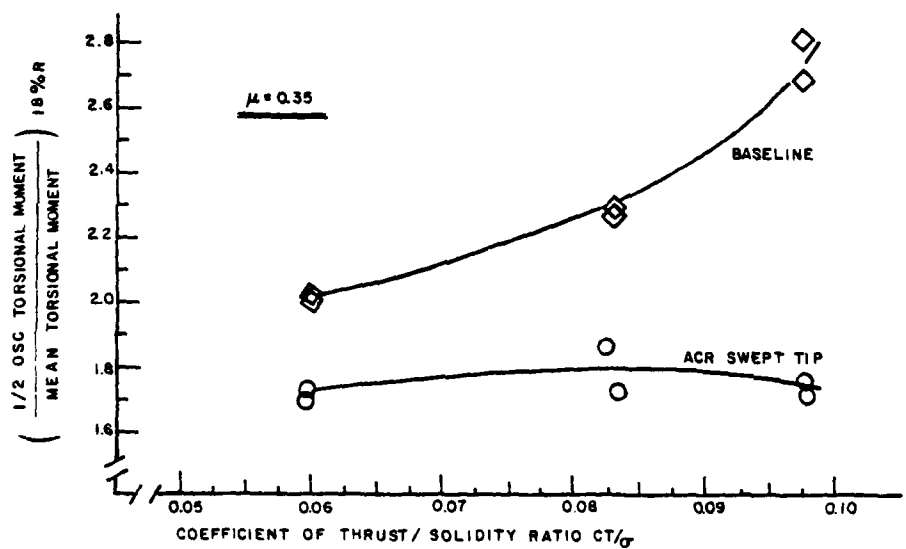
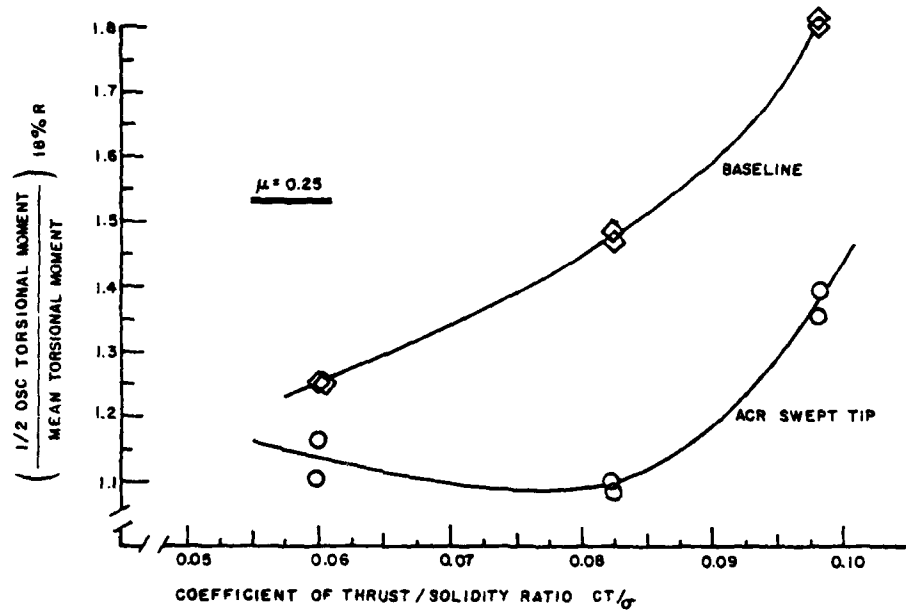


Figure 27. Oscillatory Torsional Moment vs. CT/σ for Two-Bladed Rotors.

THEORETICAL/EXPERIMENTAL CORRELATION

A very brief analysis of the correlation between experimental results and predicted results using measured blade properties was undertaken for an advance ratio of $\mu = 0.35$. The results of the predictions for the three rotor configurations are presented in Table 10. The two baseline rotor configurations chosen were associated with a nominal thrust condition and a higher thrust condition while the one ACR configuration analyzed was associated with the higher thrust condition.

If the predicted results are superimposed on the plots of the experimental data presented in Figure 17, the trend of the variation of the thrust versus torque for the baseline blades is approximately the same for both experimental and theoretical. The predicted torque for a given thrust, however, is approximately 25 percent higher than that measured. It was previously noted in the discussion of the experimental data that the ratio of C_T/C_Q measured for the baseline blades seemed high and was approximately 25 percent higher than that measured for other conventional rotor systems. Since the model torque measurements seem unrealistically low, it is not believed that the theoretical results are necessarily in error as one might first assume.

The one point for which a correlation of predicted and measured results was made for the ACR swept tip configuration also indicated that the predicted torque requirements were less than the measured value. The over-prediction of the torque, however, was only 11 percent for this configuration. It is noted from the data presented in Table 10 that a 0.60-degree change in the collective pitch angle at the three-quarter radius position used in the analysis would result in a near-perfect correlation of predicted and measured results.

As noted in Table 10 for the ACR swept-tip configuration, a set of calculations were conducted using linearized aerodynamics instead of the non-linear aerodynamics used in the previous sets of calculations. It can be seen from the results presented that the use of linearized aerodynamics, while improving the predicted performance characteristics, did not yield a significant increase in the performance results. This observation indicates that for the test condition analyzed, the rotor system was not operating near its limits. This conclusion is confirmed by the experimental data presented in Figure 17.

There was some concern during the performance of the program that since the ACR blades were designed for use with a rotor system that did not have pitch-flap coupling, the test data obtained using a rotor head system that had pitch-flap coupling might not yield the desired results. It was determined from the results of analyses conducted using the measured blade

TABLE 10. PREDICTED RESULTS USING MEASURED BLADE PROPERTIES

Configuration	Thrust (lb)	Torque (in.-lb)	Horsepower	$\frac{C_T}{\sigma}$	$\frac{C_Q}{\sigma}$	C_T/C_Q
NONLINEAR AERODYNAMICS:						
Baseline Blades	220.10	1125.10	12.230	0.04340	0.00405	10.720
Rectangular Tips						
$\Delta\theta_C = +0.57^\circ$	283.06	1243.89	13.520	0.05580	0.00447	12.480
$\Delta\theta_C = +1.14^\circ$	340.87	1358.80	14.770	0.06720	0.00490	13.710
Baseline Blades	397.70	1496.38	16.260	0.07840	0.00538	14.580
Rectangular Tips						
$\Delta\theta_C = +0.57^\circ$	437.52	1563.60	17.000	0.08630	0.00562	15.350
$\Delta\theta_C = +1.14^\circ$	467.27	1622.91	17.640	0.09215	0.00584	15.780
ACR Blade	356.65	1203.97	13.090	0.07033	0.00433	16.240
Swept Tip						
$\Delta\theta_C = +0.57^\circ$	396.17	1218.70	13.210	0.07812	0.00438	17.840
$\Delta\theta_C = +1.14^\circ$	432.76	1254.20	13.630	0.08530	0.00451	18.910
LINEARIZED AERODYNAMICS:						
ACR Blade	360.07	1106.58	12.027	0.07100	0.00398	17.840
Swept Tip						
$\Delta\theta_C = +0.57^\circ$	420.58	1098.15	11.940	0.08290	0.00395	20.987
$\Delta\theta_C = +1.14^\circ$	480.58	1109.86	12.064	0.09480	0.00399	23.760

and rotor parameters that while the pitch-flap coupling did have an affect on the results, it was only on the order of a few percent and thus did not significantly affect the predicted/experimental correlation.

Since a significant amount of theoretical/experimental correlation was not conducted, it cannot be stated whether or not the predictive analyses used were adequate to predict the performance characteristics of advanced rotor systems such as the ACR. It can be stated, however, that the design changes incorporated into the ACR blades on the basis of the results predicted by the analyses did yield a significant measured beneficial effect. The degree of the beneficial effect was close to that which was predicted.

CONCLUSIONS AND RECOMMENDATIONS

It is believed that the primary purpose of the research investigation was met. It was demonstrated both theoretically and experimentally that the use of the ACR concept can result in significant performance improvements.

The following specific conclusions and recommendations were also reached during the performance of the investigation:

1. At an advance ratio of $\mu = 0.25$, the four-bladed ACR rotor with swept tips had a significant performance benefit for C_T/σ greater than 0.10 over the baseline blade or the ACR blade with rectangular tips.
2. At an advance ratio of $\mu = 0.25$, the ACR blades with swept tips showed no effect of stall up to a C_T/σ of 0.110. It is recommended that this configuration be tested to higher thrust values to determine the limits of efficient operation.
3. At an advance ratio of $\mu = 0.25$, the two-bladed rotor configurations showed a significant performance benefit over their four-bladed counterparts. It is believed this performance benefit is due to a more favorable wake environment. It is recommended that additional data be obtained to more adequately define their performance characteristics, particularly at higher values of thrust.
4. At $\mu = 0.35$, the ACR blades with swept tips also indicated a performance benefit over the baseline blade and the ACR blade with rectangular tips. It is recommended that these configurations, particularly the ACR blades with swept tips, be tested to higher values of thrust in order to determine their practical performance limits.
5. At an advance ratio of $\mu = 0.35$, the two-bladed configurations showed significantly greater performance benefits over their four-bladed counterparts than they did at $\mu = 0.25$ for the same blade loading.
6. At $\mu = 0.35$, the two-bladed baseline blade was superior to the ACR swept-tip blades. Since this result is unexpected and different than it was at $\mu = 0.25$, it is recommended that additional data be obtained for these configurations in order to better define their performance characteristics, particularly at higher values of thrust.

7. While only a very limited theoretical/experimental correlation was undertaken, it is concluded that the predictive analysis used in this investigation might adequately predict the performance and dynamic characteristics of advanced rotor configurations such as the ACR. It is recommended that further correlation studies be conducted for the data that were obtained during this research investigation.
8. Since the data obtained during the tests indicate that some very beneficial effects were achieved with the ACR designs, it is highly recommended that the various blade configurations be more extensively tested so that sufficient data can be obtained and analyzed to determine the performance limits of the ACR designs and the design features that made these improvements realizable.

REFERENCES

1. Stewart, W., SECOND HARMONIC CONTROL OF THE HELICOPTER ROTOR, Aeronautical Research Council, R&M 2997, London, England, August 1952.
2. Arcidiacono, P. J., THEORETICAL PERFORMANCE OF HELICOPTERS HAVING SECOND AND HIGHER HARMONIC FEATHERING CONTROL, Journal of the American Helicopter Society, April 1961.
3. AN EXPERIMENTAL INVESTIGATION OF A SECOND HARMONIC FEATHERING DEVICE ON THE UH-1A HELICOPTER, Bell Helicopter Company, USATRECOM Technical Report 62-109, U.S. Army Transportation and Engineering Command, Fort Eustis, Virginia, June 1963.
4. Daughaday, H., SUPPRESSION OF TRANSMITTED HARMONIC ROTOR LOADS BY BLADE PITCH CONTROL, Cornell Aeronautical Laboratory, Inc. U.S. USAAVLABS Technical Report 67-14, U.S. Army Aviation Materiel Laboratories, Fort Eustis, Virginia, November 1967, AD 665430.
5. Balcerak, J. C., and Erickson, J. C., SUPPRESSION OF TRANSMITTED HARMONIC VERTICAL AND INPLANE ROTOR LOADS BY BLADE PITCH CONTROL, CORNELL AERONAUTICAL LABORATORY, INC., USAAVLABS Technical Report 69-39, U.S. Army Aviation Materiel Laboratories, Fort Eustis, Virginia, July 1969, AD 860352.
6. Sissingh, G. J., and Donham, R. E., HINGELESS ROTOR THEORY AND EXPERIMENT ON VIBRATION REDUCTION BY PERIODIC VARIATION OF CONVENTIONAL CONTROLS, Proceedings of the AHS/NASA-Ames Specialists' Meeting on Rotorcraft Dynamics, February 1974 (NASA SP 352, February 1974).
7. McHugh, Frank J., and Shaw, John, Jr., BENEFITS OF HIGHER HARMONIC BLADE PITCH: VIBRATION REDUCTION, BLADE- LOAD REDUCTION, AND PERFORMANCE IMPROVEMENT, American Helicopter Society Mid-East Region Symposium on Rotor Technology, August 1976.
8. Lemnios, Dr. A. Z., and Howes, H. E., WIND TUNNEL INVESTIGATION OF THE CONTROLLABLE TWIST ROTOR PERFORMANCE AND DYNAMIC BEHAVIOR, Kaman Aerospace Corporation, USAAMRDL Technical Report 77-10, Applied Technology Laboratory, U.S. Army Research and Technology Laboratories (AVRADCOM) Fort Eustis, Virginia, June 1977, AD A042481.
9. McCloud, John L., III, AN ANALYTICAL STUDY OF A MULTICYCLE CONTROLLABLE TWIST ROTOR, Proceedings of the 31st Annual National Forum of the American Helicopter Society, Washington, DC, May 1975.

10. Gabel, R., and Tarzanin, F., Jr., BLADE TORSIONAL TUNING TO MANAGE LARGE AMPLITUDE CONTROL LOADS, Journal of Aircraft, Vol. II, No. 8, Paper No. 72-958, AIAA, August 1974.
11. Kidd, D. L., Brogdon, V. H., and White, J. A., ADVANCED TWO-BLADED ROTOR SYSTEMS AT BELL HELICOPTER TEXTRON, American Helicopter Society Mid-East Region Symposium on Rotor Technology, August 1976.
12. Arcidiacono, P., and Zincone, R., UTTAS ROTOR BLADE, Journal of the American Helicopter Society, April 1976.
13. Doman, G. S., Tarzanian, F. J., and Shaw, J., Jr., INVESTIGATION OF AERO-ELASTICALLY ADAPTIVE ROTORS, Boeing Vertol Company, USAAMRDL Technical Report 77-3, Applied Technology Laboratory, U.S. Army Research and Technology Laboratories (AVRADCOR) Fort Eustis, Virginia, May 1977, AD A042083.
14. Davis, J. M., Bennett, R. L., and Blankenship, B. L., ROTORCRAFT FLIGHT SIMULATION WITH AEROELASTIC ROTOR AND IMPROVED AERODYNAMIC REPRESENTATION, Vol. 1 - Engineer's Manual, Bell Helicopter Company, USAAMRDL TR 74-10A, Eustis Directorate, U.S. Army Aviation Materiel Laboratories, Fort Eustis, Virginia, June 1974, AD 782854.
15. Blackwell, R. H., INVESTIGATION OF THE COMPLIANT ROTOR CONCEPT, Sikorsky Aircraft; USAAMRDL TR 77-7, Eustis Directorate, U.S. Army Air Mobility Research and Development Laboratory, Fort Eustis, Virginia, June 1977, AD A042338.
16. THE DEVELOPMENT AND APPLICATION OF AN ANALYSIS FOR THE DETERMINATION OF COUPLED TAIL ROTOR/HELICOPTER AIR RESONANCE BEHAVIOR, RASA Division, Systems Research Laboratories, Inc.; USAAMRDL TR 75-35, Eustis Directorate, U.S. Army Air Mobility Research and Development Laboratory, Fort Eustis, Virginia, August 1975, AD A014989.

BIBLIOGRAPHY

1. Wood, E. R., Hilzinger, K. D., and Buffalano, A. C., AN AEROELASTIC STUDY OF HELICOPTER ROTOR SYSTEMS IN HIGH SPEED FLIGHT, Sikorsky, CAL/TRECOM Symposium, "Dynamic Load Problems Associated with Helicopters and V/STOL Aircraft", Statler-Hilton, Buffalo, New York, June 26-28, 1963.
2. Leone, P. F., A NOTE ON THE EFFECTS OF LONGITUDINAL CYCLIC PITCH CONTROL VARIATIONS ON THE FORCED AEROELASTIC RESPONSE OF A HELICOPTER ROTOR BLADE, Vertol Aircraft Corporation, Journal of the American Helicopter Society, Vol. 4, No. 4, October 1959.
3. Arcidiacono, P. J., THEORETICAL PERFORMANCE OF HELICOPTERS HAVING SECOND AND HIGHER HARMONIC FEATHERING CONTROL, United Aircraft Corporation, Journal of the American Helicopter Society, Vol. 6, No. 2, April 1961.
4. Gerstenberger, W., and Wood, E. R., ANALYSIS OF HELICOPTER AEROELASTIC CHARACTERISTICS IN HIGH SPEED FLIGHT, Sikorsky Aircraft, IAS/AHS Joint Session, Institute of Aerospace Sciences, 31st Annual Meeting, Hotel Astor, New York, January 21-23, 1963.
5. Ward, J., A SUMMARY OF HINGELESS ROTOR STRUCTURAL LOADS AND DYNAMICS RESEARCH, NASA/Langley Research Center, Symposium on the Noise and Loading Actions on Helicopter, V/STOL Aircraft, and Ground Effect Machines, 1965.
6. Hohenemeser, K. H., HINGELESS ROTORCRAFT FLIGHT DYNAMICS, AGARDOGRAPH No. 197, 1974. 10
F
7. Hansford, R. E., and Simons, I. A., TORSION-FLAP-LAG COUPLING ON HELICOPTER ROTOR BLADES, Journal of the American Helicopter Society, Vol. 18, No. 4, October 1973.
8. Alexander, H. R., and Leone, P. F., V/STOL DYNAMICS AND AEROELASTIC ROTOR, Airframe Technology, Vol. 1, State-of-the-Art Review of V/STOL Rotor Technology, The Boeing Company, Vertol Division, Air Force Flight Dynamics Laboratory Technical Report 72-40, January 1973.
9. Alexander, H. R., Amos, A. K., Tarzanin, F. Jr., and Taylor, R. B., V/STOL DYNAMICS AND AEROELASTIC ROTOR, Airframe Technology, Vol. II, Description and Correlation of New Methodologies, The Boeing Company, Vertol Division, Air Force Flight Dynamics Laboratory Technical Report 72-40, September 1972.
10. White, R. P. Jr., COMMENTS AND RECOMMENDATIONS REGARDING APPLICATION OF THEORETICAL PREDICTION TECHNIQUES TO CURRENT AND ADVANCED TECHNOLOGY ROTOR SYSTEMS, RASA Division, Systems Research Laboratories, Inc., August 1976.

11. Landgrebe, A. J., Moffitt, R. C., and Clark, D. R., AERODYNAMIC TECHNOLOGY FOR ADVANCED ROTORCRAFT, National Symposium on Rotor Technology, American Helicopter Society Mid-East Region, Essington, Pennsylvania, August 1976.
12. McHugh, F. G., and Shaw, J. Jr., BENEFITS OF HIGHER HARMONIC BLADE PITCH: VIBRATION REDUCTION, BLADE-LOAD REDUCTION, AND PERFORMANCE IMPROVEMENT, The Boeing Company, Vertol Division, AHS Mid-East Region Symposium on Rotor Technology, Essington, Pennsylvania, August 1976.
13. Harvey, K. W., AEROELASTIC ANALYSIS OF A BEARINGLESS ROTOR, Bell Helicopter Company, American Helicopter Society Mid-East Region Symposium on Rotor Technology, Essington, Pennsylvania, August 1976.
14. Pei Chi Chou, PITCH-LAG INSTABILITY OF HELICOPTER ROTORS, Journal of the American Helicopter Society, Vol. 3, No. 3, July 1958.
15. Harris, F., ARTICULATED ROTOR BLADE FLAPPING MOTION AT LOW ADVANCE RATIO, The Boeing Company, Vertol Division, Journal of the American Helicopter Society, Vol. 17, No. 1, January 1972.
16. Ormiston, R. A., COMPARISON OF SEVERAL METHODS FOR PREDICTING LOADS ON A HYPOTHETICAL HELICOPTER ROTOR, U.S. Army Air Mobility Research and Development Laboratory, Moffett Field, Journal of the American Helicopter Society, Vol. 19, No. 4, October 1974.
17. Anderson, W. D., Conner, F., Kretsinger, P., and Reaser, J. S., REXOR ROTORCRAFT SIMULATION MODEL, Vol. 1-Engineering Documentation, Lockheed California Company; U.S. Army Air Mobility Research and Development Laboratory Technical Report 76-28A, Eustis Directorate, U.S. Army Air Mobility Research and Development Laboratory, Fort Eustis, Virginia, July 1976, AD A028314.
18. Rabbott, J. P. Jr., A STUDY OF THE OPTIMUM ROTOR GEOMETRY FOR A HIGH SPEED HELICOPTER, Sikorsky; U.S. Army TRECOM, Fort Eustis, Virginia, May 1962. No AD number available.
19. Blackwell, R. H., and Commerford, G. L., INVESTIGATION OF THE EFFECTS OF BLADE STRUCTURAL DESIGN PARAMETERS ON HELICOPTER STALL BOUNDARIES, Sikorsky Aircraft; U.S. Army Air Mobility Research and Development Laboratory Technical Report 74-25, Eustis Directorate, U.S. Army Air Mobility Research and Development Laboratory, Fort Eustis, Virginia, May 1977, AD 784594.
20. Cheney, M. C., Jr., RESULTS OF PRELIMINARY STUDIES OF A BEARINGLESS HELICOPTER ROTOR CONCEPT, United Aircraft Research Laboratories, Journal of the American Helicopter Society, Vol. 17, No. 4, October 1972.
21. Burkam, J. E. and Miao, Wen-Liu, EXPLORATION OF AEROELASTIC STABILITY BOUNDARIES WITH A SOFT IN-PLANE HINGELESS ROTOR MODEL, The Boeing Company, Vertol Division, Journal of the American Helicopter Society, Vol. 17, No. 4, October 1972.

22. Gaffey, T. M., THE EFFECT OF POSITIVE PITCH-FLAP COUPLING ON ROTOR BLADE MOTION STABILITY AND FLAPPING, The Bell Helicopter Company, Journal of the American Helicopter Society, Vol. 14, No. 2, April 1969.
23. Johnson, W. and Ham, N. D., ON THE MECHANISM OF DYNAMIC STALL, Journal of the American Helicopter Society, Vol. 17, No. 4, October 1972.
24. Johnson, W., THE EFFECTS OF DYNAMIC STALL ON THE RESPONSE AND AIRLOADING OF HELICOPTER ROTOR BLADES, Journal of the American Helicopter Society, Vol. 14, No. 2, April 1969.
25. Bellinger, E. D., ANALYTICAL INVESTIGATION OF THE EFFECTS OF BLADE FLEXIBILITY, UNSTEADY AERODYNAMICS, AND VARIABLE INFLOW ON HELICOPTER ROTOR STALL CHARACTERISTICS, United Aircraft Research Laboratories, Journal of the American Helicopter Society, Vol. 17, No. 3, July 1972 (NASA CR-1769, September 1971).
26. Arcidiacono, P. and Zincone, R., TITANIUM UTTAS MAIN ROTOR BLADE, Sikorsky Aircraft, Journal of the American Helicopter Society, Vol. 21, No. 2, April 1976.
27. Kidd, D. L., Spivey, R. F., and Lawrence, K. L., CONTROL LOADS AND THEIR EFFECTS ON FUSELAGE VIBRATIONS, Journal of the American Helicopter Society, Vol. 12, No. 4, October 1967.
28. Jarris, F. D., Tarzanin, F. J. Jr., and Fisher, R. K. Jr., ROTOR HIGH SPEED PERFORMANCE THEORY VERSUS TEST, The Boeing Company, Vertol Division, Journal of the American Helicopter Society, Vol. 15, No. 3, July 1970.
29. Lemnios, A. Z., and Smith, A. F., AN ANALYTICAL EVALUATION OF THE CONTROLLABLE TWIST ROTOR PERFORMANCE AND DYNAMIC BEHAVIOR, Kaman Aerospace Corporation; U.S. Army Air Mobility Research and Development Laboratory Technical Report 72-16, Eustis Directorate, U.S. Army Air Mobility Research and Development Laboratory, Fort Eustis, Virginia, May 1972, AD 747808.
30. Arcidiacono, P. J., Carta, F. O., Casellini, L. M., and Elman, H. L., INVESTIGATION OF HELICOPTER CONTROL LOADS INDUCED BY STALL FLUTTER, Sikorsky Aircraft; U.S. Army Aviation Materiel Laboratories Technical Report 70-2, U.S. Army Aviation Materiel Laboratories, Fort Eustis, Virginia, March 1970, AD 809823.
31. Carta, F. O., Commerford, G. L., Carlson, R. G., and Blackwell, R. H., INVESTIGATION OF AIRFOIL DYNAMIC STALL AND ITS INFLUENCE ON HELICOPTER CONTROL LOADS, United Aircraft Research Laboratories; U.S. Army Aviation Materiel Laboratories Technical Report 72-51, U.S. Army Aviation Materiel Laboratories, Fort Eustis, Virginia, September 1972, AD 752917.

11
B

32. Arcidiacono, P. J., PREDICTION OF ROTOR INSTABILITY AT HIGH FORWARD SPEEDS, Vol. I-Steady Flight Differential Equations of Motion for a Flexible Helicopter Blade with Chordwise Mass Balance, Sikorsky Aircraft; U.S. Army Aviation Materiel Laboratories Technical Report 68-18A, U.S. Army Aviation Materiel Laboratories, Fort Eustis, Virginia, February 1969, AD 685860.
33. Astil, C. J., and Niebanck, C. F., PREDICTION OF ROTOR INSTABILITY AT HIGH FORWARD SPEEDS, Vol. II-Classical Flutter, Sikorsky Aircraft; U.S. Army Aviation Materiel Laboratories Technical Report 68-18B, U.S. Army Aviation Materiel Laboratories, Fort Eustis, Virginia, February 1969, AD 685861.
34. Niebanck, C. F., and Elman, H. L., PREDICTION OF ROTOR INSTABILITY AT HIGH FORWARD SPEEDS, Vol. IV-Torsional Divergence, Sikorsky Aircraft; U.S. Army Aviation Materiel Laboratories Technical Report 68-18D, U.S. Army Aviation Materiel Laboratories, Fort Eustis, Virginia, February 1969, AD 687323.
35. Charles, B. D., AN EXPERIMENTAL/THEORETICAL CORRELATION OF MODEL AND FULL-SCALE ROTOR PERFORMANCE AT HIGH ADVANCING-TIP MACH NUMBERS AND HIGH ADVANCE RATIOS, Bell Helicopter Company; U.S. Army Aviation Materiel Laboratories Technical Report 70-69, U.S. Army Aviation Materiel Laboratories, Fort Eustis, Virginia, January 1971, AD 881982.
36. Ericsson, L. E., and Reding, J. P., DYNAMIC STALL OF HELICOPTER BLADES, Lockheed Missiles and Space Company, Journal of the American Helicopter Society, Vol. 17, No. 1, January 1972.
37. Ormiston, R. A., and Bousman, W. G., A STUDY OF STALL-INDUCED FLAP-LAG INSTABILITY OF HINGELESS ROTORS, Journal of the American Helicopter Society, Vol. 20, No. 1, January 1975.
38. Sissingh, Dr. G. J., DYNAMICS OF ROTORS OPERATING AT HIGH ADVANCE RATIOS, Lockheed California Company, Journal of the American Helicopter Society, Vol. 13, No. 3, July 1968.
39. Briczinski, S. J., VALIDATION OF THE ROTORCRAFT FLIGHT SIMULATION PROGRAM (C81) FOR ARTICULATED ROTOR HELICOPTERS THROUGH CORRELATION WITH FLIGHT DATA, Sikorsky Aircraft; U.S. Army Air Mobility Research and Development Laboratory Technical Report 76-4, Eustis Directorate, U.S. Army Air Mobility Research and Development Laboratory, Fort Eustis, Virginia, May 1976, AD A025934.
40. Staley, J. A., VALIDATION OF ROTORCRAFT FLIGHT SIMULATION PROGRAM THOROUGH CORRELATION WITH FLIGHT DATA FOR SOFT-IN-PLANE HINGELESS ROTORS, Boeing Vertol Company; U.S. Army Air Mobility Research and Development Laboratory Technical Report 75-50, Eistis Directorate, U.S. Army Air Mobility Research and Development Laboratory, Fort Eustis, Virginia, January 1976, AD A021176.

41. Freeman, F. D., and Bennett, R. L., APPLICATION OF ROTORCRAFT FLIGHT SIMULATION PROGRAM (C81) TO PREDICT ROTOR PERFORMANCE AND BENDING MOMENTS FOR A MODEL FOUR-BLADED ARTICULATED ROTOR SYSTEM, Bell Helicopter Company; U.S. Army Air Mobility Research and Development Laboratory Technical Report 74-70, Eustis Directorate, U.S. Army Air Mobility Research and Development Laboratory, Fort Eustis, Virginia, November 1974, AD A00415.
42. Johnston, R. A., and Cassarino, S. J., AEROELASTIC ROTOR STABILITY ANALYSIS, Sikorsky Aircraft; U.S. Army Air Mobility Research and Development Laboratory Technical Report 75-40, Eustis Directorate, U.S. Army Air Mobility Research and Development Laboratory, Fort Eustis, Virginia, January 1976, AD A020871.
43. Hoffstedt, D. J., ADVANCED GEOMETRY, GLASS-FIBER-REINFORCED PLASTIC ROTOR BLADE TEST PROGRAM, The Boeing Company, Vertol Division; U.S. Army Air Mobility Research and Development Laboratory Technical Report 71-42, Eustis Directorate, U.S. Army Air Mobility Research and Development Laboratory, Fort Eustis, Virginia, September 1971, AD 738203.
44. Burkam, J. E., Capurso, V., and Yntema, R. T., A STUDY OF THE EFFECT OF SYSTEMATIC VARIATIONS OF ROTOR BLADE PLANFORM, TWIST, AND MASS DISTRIBUTION ON HUB LOADS FOR A THREE-BLADED HELICOPTER ROTOR, Vertol Aircraft Corporation, July 1959.
45. McKenzie, K. T., and Howell, D.A.S., THE PREDICTION OF LOADING ACTIONS ON HIGH SPEED SEMI-RIGID ROTOR HELICOPTERS, AGARD Specialists Meeting on Helicopter Rotor Loads Prediction Methods, Milano, Italy, March 1973.
46. Bielawa, R. L., AEROELASTIC CHARACTERISTICS OF COMPOSITE BEARINGLESS ROTOR BLADES, Sikorsky Aircraft, 32nd Annual National Forum of the American Helicopter Society, Washington, DC, May 1976.
47. Sutton, L. R., Gangwani, S. T., and Nettles, W. E., ROTOR/HELICOPTER SYSTEM DYNAMIC AEROELASTIC STABILITY ANALYSIS AND ITS APPLICATION TO A FLEXSTRAP TAIL ROTOR, 32nd Annual National Forum of the American Helicopter Society, Washington, DC, May 1976.
48. Daughaday, H., SUPPRESSION OF TRANSMITTED HARMONIC ROTOR LOADS BY BLADE PITCH CONTROL, Cornell Aeronautical Laboratory; U.S. Army Aviation Materiel Laboratories Technical Report 67-14, November 1967.
49. White, R. P. Jr., VTOL PERIODIC AERODYNAMIC LOADINGS: THE PROBLEMS, WHAT IS BEING DONE AND WHAT NEEDS TO BE DONE, Cornell Aeronautical Laboratory, Journal of Sound Vibrations, (1966) 4(3), pp. 202-304.
50. Curtiss, H.C., Jr., and Shupe, N.K., A STABILITY AND CONTROL THEORY FOR HINGELESS ROTORS, 27th Annual Forum of the American Helicopter Society, May 1971.
51. Miao, Wen-Liu, and Huber, H., ROTOR ELASTICITY COUPLED WITH HELICOPTER BODY MOTION. Specialists Meeting on Rotorcraft Dynamics, Moffett Field, California, February 1974.

52. Taylor, R., Fries, J., and MacDonald, H. I., Jr., REDUCTION OF HELICOPTER CONTROL SYSTEM LOADS WITH FIXED SYSTEM DAMPING, 29th Annual Forum of the American Helicopter Society, Washington, DC, Preprint No. 773, May 1973.
53. HELICOPTER ROTOR HUB VIBRATORY FORCES SYSTEMATIC VARIATION OF FLEXIBLE ROTOR BLADE PARAMETERS, The Boeing Company, Vertol Division; prepared under Navy Bureau of Weapons Contract No. A(S)60-6112C, May 1961.
54. Blackwell, R. H., Murrill, R. J., Yeager, W. T., Jr, and Mirick, P., WIND TUNNEL EVALUATION OF AEROELASTICALLY CONFORMABLE ROTORS, Journal of the American Helicopter Society, Vol. 26, No. 2, April 1981.

LIST OF SYMBOLS

AC	Aerodynamic Center
CG	Center of Gravity
C_{M0}	Pitching Moment Coefficient due to Camber
C_Q	Rotor Torque Coefficient $Q/\pi R^2 (\Omega R)^2 R$
C_T	Rotor Thrust Coefficient $T/\pi R^2 (\Omega R)^2$
F_D	Drag Force lb
F_S	Side Force lb
Hz	Hertz-cycles/sec
M_N	Mach Number
M_P	Pitching Moment-in.-lb
M_R	Rolling Moment-in.-lb
M_Y	Yaw Moment-in.-lb
N_F	Normal Force-lb
Q	Rotor Torque-in.-lb
q	Dynamic Pressure -lb/in ²
R	Rotor Radius -in.
r	Local rotor radius in.
RPM	Revolutions Per Minute
T	Rotor thrust-lbs
V	Free Stream Velocity-in./sec
$\Delta\theta_C$	Increment in Collective Pitch Angle - deg
μ	Advance Ratio
ρ	Density of Air-slugs/in.
σ	Rotor Solidity-ratio of the total blade area to the rotor disc area
Ω	Rotor Rotational Speed-rad/sec

DATE
ILME